

<https://doi.org/10.11646/zootaxa.5501.2.1>

<http://zoobank.org/urn:lsid:zoobank.org:pub:4112F569-8CC4-401E-9837-0C0F6F8C4F66>

The species of *Pteromalus* Swederus in America north of Mexico with a 4:4 mandibular formula, and description of a potential biocontrol agent of the introduced pest *Anthonomus rubi* (Herbst) (Coleoptera: Curculionidae)

GARY A. P. GIBSON¹, YONATHAN URIEL^{2,9}, JADE SHERWOOD³, PAUL K. ABRAM^{2,10}, TARA D. GARIEPY⁴, Y. MILES ZHANG⁵, HANNES BAUR^{6,7}, MICHAEL GATES⁸ & MICHELLE T. FRANKLIN^{2*}

¹Honorary Research Associate, Agriculture and Agri-Food Canada, Canadian National Collection of Insects, Arachnids and Nematodes, K. W. Neatby Bldg., 960 Carling Avenue, Ottawa, Ontario, CANADA, K1A 0C6.

 gary.gibson@agr.gc.ca;  <https://orcid.org/0000-0002-8161-7445>

²Agriculture and Agri-Food Canada, Agassiz Research and Development Centre, 6947 Hwy 7, Agassiz, British Columbia, CANADA, V0M 1A0.

³University of British Columbia, Department of Lands and Food Systems, 248-2357 Main Mall, Vancouver, BC, CANADA, V6T 1Z4.

 jadee.sherwood@yahoo.ca;  <https://orcid.org/0009-0008-8302-6359>

⁴Agriculture and Agri-Food Canada, London Research and Development Centre, 1391 Sandford Street, London, Ontario, CANADA, N5V 4T3.

 tara.gariepy@agr.gc.ca;  <https://orcid.org/0000-0003-2533-3023>

⁵Institute of Ecology and Evolution, University of Edinburgh, Charlotte Auerbach Road, Edinburgh, EH9 3FL, UK.

 yuangmeng.zhang@gmail.com;  <https://orcid.org/0000-0003-4801-8624>

⁶Natural History Museum Bern, Bernastrasse 15, 3005 Bern, Switzerland.

 hannes.baur@nmbe.ch;  <https://orcid.org/0000-0003-1360-3487>

⁷Institute of Ecology and Evolution, University of Bern, Baltzerstrasse 6, 3012 Bern, Switzerland.

⁸Systematic Entomology Laboratory, USDA-ARS, c/o NMNH, Smithsonian Institution, 10th & Constitution Avenue, NW, Washington, DC, USA, 20013-7012.

 michael.gates@usda.gov;  <https://orcid.org/0000-0002-5760-1371>

⁹ yonathan.uriel@agr.gc.ca;  <https://orcid.org/0000-0003-3086-2069>

¹⁰ paul.abram@agr.gc.ca;  <https://orcid.org/0000-0002-8564-6227>

*Corresponding author:  [michelle.franklin@agr.gc.ca](mailto: michelle.franklin@agr.gc.ca);  <https://orcid.org/0000-0002-5699-437X>

Abstract

The strawberry blossom weevil, *Anthonomus rubi* (Herbst) (Coleoptera: Curculionidae), is native to Europe, Asia, and parts of North Africa, and has recently established in British Columbia, Canada and Washington State, USA. To determine whether any parasitoids in British Columbia parasitize this recently-established pest, *A. rubi*-infested buds of Rosaceous host plants were collected and reared for parasitoid emergence. *Pteromalus quadridentatus* Gibson n. sp. (Hymenoptera: Chalcidoidea: Pteromalidae) is described from both sexes reared as solitary ectoparasitoids of *A. rubi*. Males and females are partly characterized by both mandibles having four teeth (4:4 mandibular formula), which is known for only four of the other previously recorded 39 extant species of *Pteromalus* from the Nearctic region—*P. apum* (Retzius), *P. cassotis* Walker, *P. hemileucae* Gahan, and *P. puparum* (L.). The species of *Pteromalus* recorded from the Nearctic region are listed along with notes on their known mandibular dentition or other features that differentiate them from *P. quadridentatus*. The five species with a 4:4 mandibular formula are keyed, diagnosed and illustrated through macrophotography. Additionally, both sexes of *P. quadridentatus* are described more comprehensively, including variation in structure, colour and sculpture correlated with body size; the morphological species limits of *P. cassotis* are also discussed. Species of *Pteromalus* with a 4:4 mandibular formula from other regions where *A. rubi* is recorded are also listed and discussed, but only sufficiently to exclude them as potentially conspecific with *P. quadridentatus*. A phylogenetic tree constructed using Maximum Likelihood based on COI barcode sequences showed strong support for *P. quadridentatus* being monophyletic and sister to *P. bedeguaris* (Thomson). *Pteromalus quadridentatus* is the first parasitoid recorded from *A. rubi* in its invaded range, although it is still uncertain whether this parasitoid is native to North America or was introduced along with *A. rubi* or another host species.

Key words: Chalcidoidea, taxonomy, strawberry blossom weevil, COI barcode, phylogeny, species delimitation

Introduction

The establishment of strawberry blossom weevil, *Anthonomus rubi* (Herbst) (Coleoptera: Curculionidae) was first reported in North America in the Greater Vancouver area and Fraser Valley, British Columbia, Canada in 2019 (Franklin *et al.* 2021). Since then, it has also been reported from Washington State, USA, near the Canada-USA border (Roueché *et al.* 2022). The species is known also from Europe, Asia, and parts of North Africa (Alonso-Zarazaga *et al.* 2017), but the exact area of origin and pathway(s) of entry into North America remain unknown. The species is a pest of various Rosaceae, including economically important species such as strawberries (*Fragaria* L.), raspberries (*Rubus idaeus* L.) and other *Rubus* species, including the invasive Himalayan blackberry (*Rubus armeniacus* Focke), and *Rosa* species (Franklin *et al.* 2021; Roueché *et al.* 2022). In addition to recording *A. rubi*, Franklin *et al.* (2021) reported at least one species of *Pteromalus* Swederus (Hymenoptera: Pteromalidae) as a parasitoid of *A. rubi* in British Columbia. Biological control with native and/or exotic parasitoid natural enemies has the potential to contribute to pest management programs for *A. rubi*, which motivated our effort to determine the identity of the parasitoid and its geographic origins.

Noyes (2019) listed 39 valid, extant species of *Pteromalus* from the Nearctic region. The only taxonomic revision for the Nearctic region is for North America north of Mexico by Girault (1917). Girault (1917) treated 11 species of *Pteromalus* characterized by a 3:4 mandibular formula (three teeth on left mandible and four teeth on right mandible) under the generic name *Habrocytus* Thomson. Graham (1969, p. 489) noted that “*Habrocytus* is extremely close to *Pteromalus*, and it is a matter of opinion whether the two should be united or not”. Species of *Pteromalus sensu stricto* are characterized by both mandibles having four teeth (4:4 mandibular formula). The number of teeth on each mandible has not been evaluated as a reliable phylogenetic indicator, but at least it is not a very good key character because when the mandibles are closed the dentition of the left mandible often is not visible. Because of this, even though Graham (1969) treated the species of *Pteromalus* and *Habrocytus* separately, he keyed them together within a single key. Graham (1969, p. 495) also stated that although “rarely aberrations [in the number of teeth] occur”...“the number of teeth appears to be very constant within the species”. Thus, even if not a good key character because of visibility, it is an important differential feature to be considered for species recognition. Bouček & Graham (1978) synonymized *Habrocytus* under *Pteromalus*, which was followed by Noyes (2019). Some authors subsequent to Bouček & Graham (1978) retained the two names as valid genera (e.g. Burks 1979; Liao *et al.* 1987) or treated *Habrocytus* as a subgenus of *Pteromalus* (e.g. Dzhanokmen 1998, 2001), but we do not recognize subgenera and treat *Habrocytus* as a synonym of *Pteromalus*.

Described species of *Pteromalus* with a 4:4 mandibular formula appear to be far fewer in number than those with a 3:4 formula. For example, of the 67 species Graham (1969) treated from northwestern Europe, eight named species were reported under *Pteromalus* and 59 named species under *Habrocytus* (12%). Of the 39 extant described species of *Pteromalus* recorded from the Nearctic by Noyes (2019), only four (10%) are characterized by a 4:4 mandibular formula—*P. apum* (Retzius), *P. cassotis* Walker, *P. hemileucae* Gahan, and *P. puparum* (L.). All four species are gregarious parasitoids, of which *P. cassotis* and *P. hemileucae* are Nearctic or New World in distribution, whereas *P. apum* and *P. puparum* are known also from the Palaearctic (Noyes 2019). Consequently, the latter two species either are naturally occurring Holarctic species or were introduced into North America accidentally sometime in the past. It is also uncertain whether the new species of *Pteromalus* described herein is native to North America or was introduced from elsewhere along with *A. rubi* or, perhaps, with some other previously introduced weevil. However, our present investigations indicate that the species is new to science and we describe it at this time because a name is required to report the results of ongoing research related to the ecology and biological control of *A. rubi*.

Material and methods

Material. Codes used in the text for the collections housing specimens treated in this study are as follows:

CNC	Canadian National Collection of Insects, Arachnids and Nematodes, Agriculture and Agri-Food Canada, Ottawa, ON, Canada.
NMBE	Natural History Museum Bern, Bern, Switzerland.

- NHMUK** The Natural History Museum (formerly British Museum of Natural History), Department of Life Sciences, London, England.
- ULQC** Collection Léon Provancher, Université Laval, Québec, QC, Canada.
- USNM** National Insect Collection, National Museum of Natural History, Smithsonian Institution, Washington, DC, USA.

Specimen rearing. Severed, fully closed pre-bloom flower buds were collected from strawberry (*Fragaria* L.), shrubby cinquefoil (*Dasiphora fruticosa* L), raspberry (*Rubus ideaeus* L.), and Himalayan blackberry (*Rubus armeniacus* Focke) during the 2020–2023 growing seasons at several sites throughout the Fraser Valley and Metro Vancouver region, Canada (Fig. 1). In 2023, damaged buds were also collected from northern Washington State, USA following the same procedure (Fig. 1). Clipped buds were kept in 250 mL mesh-top BugDorm containers (MegaView Science co., Taichung, Taiwan) in an outdoor shelter or indoors in a temperature-controlled chamber (20–22 °C). Buds were misted every two to three days to maintain high humidity. Containers were monitored for emergence of parasitoids two to three times per week and parasitoids were collected into vials containing 95% ethanol. A subset of buds were dissected and examined for the presence of larval parasitoids. Larval parasitoids were placed into petri dishes and monitored for pupation and emergence.

Morphological description. Specimens designated as type material of the newly described species were sent in ethanol to the CNC where they were critical-point dried and point-mounted by GAPG. Specimens were then examined using a Nikon SMZ-U microscope fitted with a 10 mm ocular grid having 100 divisions for measurements, and a Leitz 100-watt tungsten halogen light source was used for illumination. A piece of translucent Mylar tracing acetate was taped to the objective between the light source and specimen to reduce glare. Images of the lectotype and paralectotype of *P. cassotis* were provided by Natalie Dale-Skey (NHMUK), and of the lectotypes of *P. fuscipes* (Provancher) and *P. melanicus* (Provancher) (ULQC) by Joseph Moisan-De Serres (Ministère de l’Agriculture, des Pêcheries et de l’Alimentation du Québec, Québec, Canada). Other images were taken by GAPG using a Leica DMC5400 20 megapixel digital camera attached to a Leica Z16 APO motorized macroscope and illuminated with three Leica KL2500 LCD fibre optic light sources fitted with 250-watt cold light reflector lamps. Light was filtered through a Styrofoam dome to reduce glare. Serial images were combined with Zerene Stacker and digitally retouched as necessary using Adobe Photoshop to enhance clarity. The described colour patterns are from specimens examined with the Nikon microscope and may not always match exactly the plate images. This is because the visual appreciation of colours, metallic lusters, and their intensity is affected by several factors, including not only the condition of museum specimens of various ages but also the type of light used to examine or image a specimen (Gibson 2020). Because of artefacts that can affect colour appreciation, colour pattern, i.e. the pattern of dark versus pale or of different regions of colour on the body is often more reliable than colour itself. When the term “pale” is used this refers to a typically white to yellowish, but conspicuously lighter region than surrounding regions.

For the new species description, ratios and measurements provided, other than body length, are relative, with ranges based on measurements of 10 individuals that include some of the largest and smallest individuals. For the female description of the new species, the holotype is included as one of the specimens and its values are given between square brackets, either as part of the range if the minimum or maximum value, or following the range if within the cited range for the species. Except for the holotype, measurements or ratios were rounded to two decimal points if the value is less than one, but to only one decimal point if the value was greater than one. Males resemble females in most morphological features. Therefore, the male description includes only differences relative to the female. Measurements of described features were made mostly as described by Baur (2015, table 1, with additions as provided by Klimmek & Baur 2018). However, body length was measured in lateral view, anteriorly from the level of the toruli (when the head is directed in the plane of the body and held vertically) to the end of the ovipositor sheaths. Body length is difficult to measure accurately because in different specimens the head and gaster are often held at different angles and positions relative to the mesosoma. Further, the length of the gaster is affected by telescoping of the segments, the difference typically being the greatest between air dried (often shrivelled) and critical-point dried (often somewhat inflated) specimens. As noted by Baur (2015), it is important when taking any measurement that the two points of reference of a structure be in perfect focus to avoid errors of parallax, which is more difficult for smaller individuals and for convex structures whose two end points may be on a different plane. Because of parallax, imaging body parts at an angle and subsequent montaging of multiple images to produce a single focused image can also introduce colour artefacts or affect apparent relative proportions of structures.

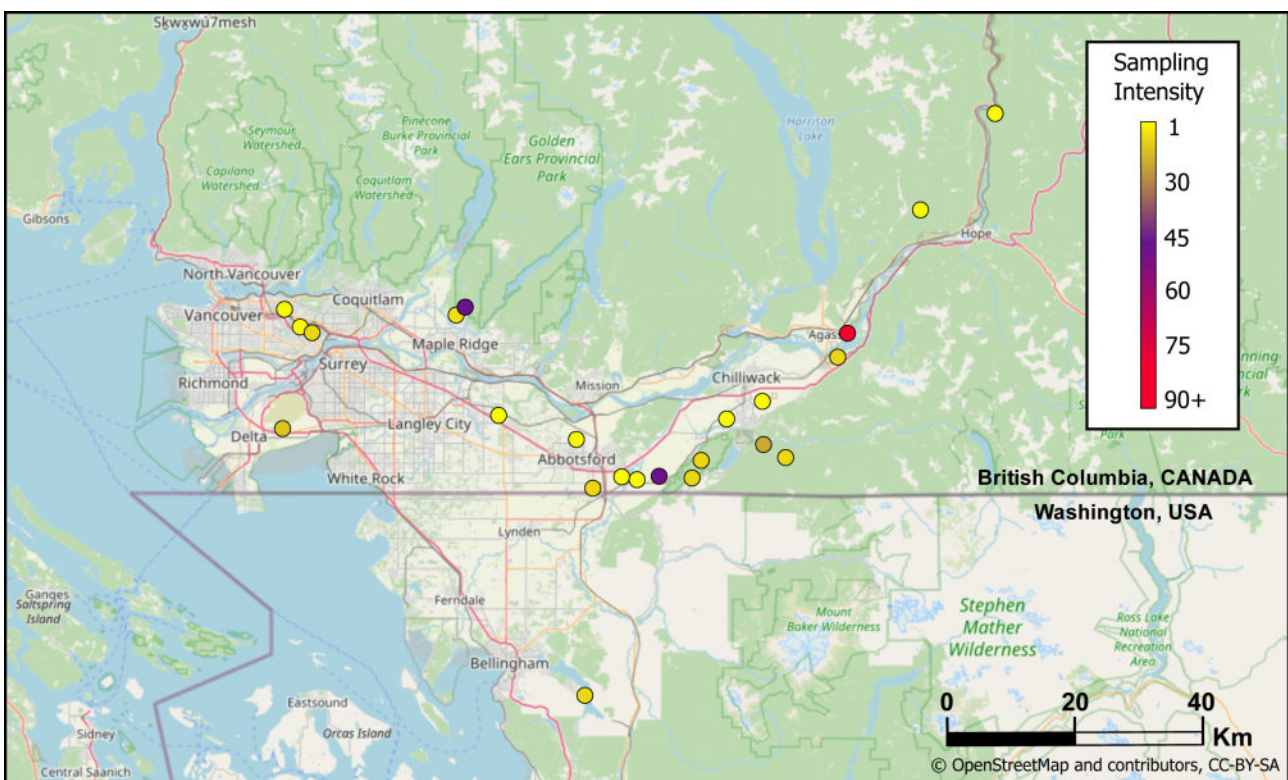


FIGURE 1. Map showing the locations in British Columbia, Canada and Washington State, USA where *Pteromalus quadridentatus* was found associated with collected buds damaged by *Anthonomus rubi*. The sampling intensity depicted by the colours represented in the legend shows the number of *P. quadridentatus* (1 to 90+) that were collected from each of the sampling sites.

Morphological terms and their abbreviations largely follow those listed and defined in Gibson (2020), other than pteromalid-specific features, which follow Graham (1969) and/or Baur (2015). The basal two flagellomeres of the antenna are strongly transverse and without **multiporous plate sensilla (mps)**, and thus are termed **anelli**, whereas the subsequent six pre-claval flagellomeres are designated as **fu1–fu6** and collectively referred to as the **funicle**. Length of the scape excludes the radicle; pedicel length is dorsal (longest) length, width of flagellomeres does not include projecting setae, and, for males, length of fu6 and the clava excludes the basal pedicel, if visible. The ventral surface of the male scape of some *Pteromalus* species has a differentiated convex sensory region that is called the **boss** (Fig. 15D,F,G). Length of the **submarginal vein** (Fig. 13D,H: **smv**) includes the **parastigma** (Fig. 13H: **pst**), the slightly thickened apical part of the submarginal vein that extends, obliquely, to the base of the marginal vein. The **marginal vein** (Fig. 13D,H: **mv**) was typically measured from the apical margin of the **hyaline break** (Fig. 13D: inset, **hb**) that delimits the apex of the parastigma and abrupt/vertical basal margin of the marginal vein to the angle formed between the **stigmal vein** (Fig. 13D: **stv**) and **postmarginal vein** (Fig. 13D: **pmv**). When the hyaline break was not distinct the basal limit of the marginal vein was interpreted as the slight constriction (Fig. 13H: **cst**) or apical-most campaniform sensilla at the abrupt base of the marginal vein, which indicate the point of juncture between the parastigma/submarginal vein and marginal vein. This measurement method of the marginal vein closely approximates that of Graham (1969), which was measured from the point at which the **costal cell** (Fig. 13D: **cc**) joins the marginal vein. However, the latter method is inexact because the costal cell membrane usually extends, very narrowly, for some distance beyond the apparent base of the marginal vein (Fig. 13D: **mb**, inset) and it is often difficult to determine the exact point of intersection. The hyaline break or campaniform sensilla are therefore used because these or the abruptly angled basal margin of the marginal vein usually are more obvious. Measurement of the costal cell is from the v-like notch at the junction of the humeral plate and base of the costal cell to the point where the base of the marginal vein was measured. Length of the postmarginal and stigmal veins are as per Graham (1969) and Baur (2015), i.e. from the angle formed between the postmarginal and stigmal vein to the apices of both, respectively. Measurements of lengths of the marginal, postmarginal and stigmal veins were taken along the

leading (outer) margins of the veins as per Graham (1969); however, in some instances the length of the marginal vein is compared to that of the stigmal vein measured along their inner margins. These additional measurements are included because they more accurately reflect the apparent (visual) length of the marginal and stigmal veins when the two veins are of similar length. Ratios of the cc: mv: stv: pmv are relative to the stigmal vein, which is assigned a value of one. Important fore wing setae (e.g. Figs 4C,D, 13D) for species differentiation include the presence of dorsal setae (**ds**) and/or ventral setae (**vs**) on the **basal fold** (Fig. 13H: **bf**), **mediocubital fold** (Fig. 13H: **mcf**), **basal cell** (Fig. 13H: **bc**) and fore wing **disc** (region of the wing membrane beyond the basal fold), and the presence of a partial (Fig. 4C) to complete (Fig. 4D) **costal setal line (csl)** on the ventral surface of the **costal cell** (Figs 4D, 13D: **cc**). The dorsally bare region of the disc beyond the basal fold behind the parastigma and marginal vein is the **speculum** (Fig. 4C,D: **spc**), which is less obvious if there are setae on the ventral surface (Fig. 4C,D). On the two-dimensional plates of illustrations, dorsal setae point upwards or obliquely toward the leading/apical margin of the wing whereas ventral setae point more or less downward (e.g. Figs 4C,D, 13H). Length of the female gaster was made either in dorsal or lateral view, depending on which view was better for taking the measurement—in dorsal view from the anterolateral margin of the gaster to the apex of the ovipositor sheaths, and in lateral view anteriorly from the vertical, lateral margin just in front of the basolateral setae of the first gastral tergite. Baur (2015) measured head height in frontal view from the ventral margin of the anterior ocellus to the apical margin of the clypeus, and compared this to head width, the greatest width measured in dorsal view (**HW**). In the new species we include this measurement as **HH: HW(B)** so as to be comparable with other species treated in Baur (2015), but also include **HH: HW**, which is the same as the previous ratio except head height (**HH**) is measured in frontal view from the top of the head to the ventral margin of the clypeus laterally, which more accurately reflects the visual appearance of the head. Head length (**HL**) is the maximum length measured in lateral view. Additional head measurements include the interocular distance (**IOD**: minimum distance between inner orbits in dorsal view), ocellocular line (**OOL**: minimum distance between a posterior ocellus and inner orbit), postocellar line (**POL**: minimum distance between the posterior ocelli), and lateral ocellar line (**LOL**: minimum distance between a posterior ocellus and anterior ocellus). The propodea of all treated species are quite similar in structure and sculpture, consisting of an anteromedian pair of **lateral panels** (Fig. 14D: **lp**) and a posterior, convex, transverse-quadrangular **nucha** (Fig. 14D: **nu**) that laterally are delineated from the **callar region** (14D: **cr**) by the **plicae** (Fig. 14D: **pl**). The lateral panels and nucha are separated by a **nuchal furrow** (Fig. 14D: **nuf**) whereas the callar region is subdivided by a **postspiracular furrow** (Fig. 14D: **psf**) behind the spiracle into a narrow region lateral to the lateral panel and a more lateral **callus** (Fig. 14D: **ca**), the only part of the propodeum with setae.

Terms for sculpture follow Gibson (2021), including **meshlike reticulate** (more or less isodiametric cells formed by raised ridges with the surface of the cell within flat), **meshlike coriaceous** (similar shaped sculpture as reticulate, but the flat-surfaced cells delineated by engraved lines rather than ridges), **pustulate** (similar shaped sculpture as coriaceous but the engraved lines comparatively deep such that the surface of the cell is convex rather than flat), **alutaceous** (coriaceous sculpture that is noticeably lengthened in one direction, typically transversely), and **imbricate** (sculpture similar to coriaceous but with one side of the cell higher than the opposite side so that the cells appear to overlap in a shingle-like manner). Sculpture consisting of fine longitudinal ridges is termed **striate** if the ridges are essentially straight (e.g. Fig. 4A,B: clypeal sculpture) but **strigose** if the ridges are more irregular, more or less wrinkled (e.g. Fig. 14D: oblique lines on lateral panels), and **crenulate** if the ridges are strong, subparallel and comparatively short (e.g. Fig. 14D: vertical ridges along anterior margin of lateral panels or transverse ridges within psf). The different sculptural extremes often intergrade and hyphenating any two indicates an intermediate sculpture (e.g. imbricate-reticulate indicates a more or less shingle-like sculpture in which the cell surface is depressed or dimpled rather than being flat).

The diagnoses of the five treated species do not repeat the features listed in the diagnosis given for regional species with a 4:4 mandibular formula, though the species description of the new species includes all features. For the four previously described species with a 4:4 mandibular formula, our concept of *P. apum* and *P. puparum* are based on Graham (1969), identified specimens in the CNC, and barcoded specimens borrowed from CBG, whereas our concept of *P. hemileucae* is based on the original description and examination of type material in the USNM, and that of *P. cassotis* based on the original description, images of type specimens provided by Natalie Dale-Skey (NHMUK), and identified specimens in the CNC and the USNM. Only diagnoses and general distribution and host data are provided for the latter four species because no attempt was made to borrow and examine all available specimens from different collections to comprehensively revise these species.

In the list of type material for the new species, the BOLD ID code of each sequenced individual is included between square brackets, but this information does not form part of the printed label data.

Molecular analysis. The left middle leg was removed from each specimen, the ethanol allowed to evaporate, and then placed in a 1.5 mL tube of 1% phosphate-buffered saline, and homogenized using a TissueLyser LT (QIAGEN, Hilden, Germany). Pancreatic ribonuclease A (RNaseA, 4 µL at 100mg/mL; QIAGEN) was added to each sample to digest RNA. Genomic DNA was then extracted using the DNeasy Blood & Tissue Kit (QIAGEN) automated on the QIAcube Connect platform (QIAGEN) using a modified program, with reduced elution volumes (2 x 50 µL of Buffer AE) to increase the DNA sample concentrations. The quantity of genomic DNA was quantified using a Qubit 4 fluorometer (ThermoFisher Scientific, Massachusetts, USA).

Previous amplification and sequencing of the Chalcidoidea showed inconsistent amplification and sequencing success using the universal barcode primers, LCO 1490 / HCO 2198 (Folmer *et al.* 1994), in particular the forward direction (Gariepy, unpublished). To improve amplification and sequencing success a set of primers nested within the standard COI DNA barcoding region were designed. To do this, DNA sequences for several species of chalcidoid parasitoids (generated from a separate project on parasitoids associated with cabbage seedpod weevil; Gariepy, unpublished) were aligned using CODONCODE ALIGNER version 9.0.1 (Codon-Code Corporation, Centerville, Massachusetts, USA). This included the following Pteromalidae: *Lycus perdubius* Girault, *Chlorocytus* Graham sp., *Stenomalina gracilis* Walker, *Trichomalus lucidus* Walker, *T. perfectus* Walker, *Mesopolobus moryoides* Gibson, *M. gemellus* Baur & Muller, *M. incultus* Walker, *Trimeromicrus maculatus* Gahan, and *Pteromalus* sp. (Genbank accession numbers no. PP495365–PP495374). Visual inspection of the aligned sequences allowed identification of areas of sequence similarity between the different species, and these areas were targeted for development of general primers for pteromalids. Two degenerate primers were developed—a forward primer (Pter-77degF) and a reverse primer (Pter-638degR) (Table 1); Pter-77degF can be used in combination with either HCO-2198 (yielding a 553-bp product) or Pter-638degR (yielding a 539-bp product). The new primers were imported into Primer3Plus (Untergasser *et al.* 2012) to confirm their suitability (i.e., stability, melting temperature, potential for hairpins, primer dimers) and determine the appropriate temperature for amplification of the desired PCR product.

TABLE 1. General Pteromalidae forward and reverse primers nested with the COI DNA barcode region.

Primer Name	Direction	Primer sequence (5' – 3')
Pter-77degF	Forward	GGDAATCCHGGDTCWTTAATTGG
Pter-638degR	Reverse	ATARRATWGGRTHCCYCCCHCC

Pter-77degF paired with reverse universal primer HCO 2198 was used for amplification and sequencing of 90% of specimens and the remaining 10% were amplified and sequenced with Pter-77degF and Pter-638degR. Attempts were made to sequence the COI region of museum specimens of *P. cassotis* and *P. hemileucae* held at the CNC and USNM; however, sequences failed or were too low quality, likely due to the age of specimens. Each PCR reaction contained 20–30 ng genomic DNA, 0.2 nM dNTP, 10 pM of each primer (Integrated DNA Technologies, Toronto, ON, Canada), 0.4 Units of Phusion High-Fidelity DNA polymerase (ThermoFisher Scientific), 20 µM Betaine, and 1X HF buffer (ThermoFisher Scientific) to bring the reaction volume to 20 µL. The PCR cycling conditions were as follows: 1× [30 sec at 98 °C], 35× [10 sec at 98 °C; 30 sec at 55 °C; 30 sec at 72 °C], 1× [5 min at 72 °C]. PCR products were purified using ExoSAP-IT (ThermoFisher Scientific) and were sequenced bi-directionally at the Applied Genomics Center, Kwantlen Polytechnic University, Surrey, BC, Canada on a SeqStudio platform (ThermoFisher Scientific). The resulting AB1 files were cleaned and aligned using Sequencher 5.4.6 (Gene Codes Corporation, Michigan, USA) and deposited in BOLD and NCBI GenBank (see Table S1).

All of the sequenced specimens were collected from within the Fraser Valley and Metro Vancouver regions, within an area approximately 120 km by 30 km in size. In addition to the individuals we sequenced, COI sequences of other identified *Pteromalus* species were obtained from other sources (Table S1) and included along with another Pteromalini species *sensu* Burks *et al.* (2022), *Nasonia vitripennis* (Walker), as the outgroup for the phylogenetic analyses. The phylogenetic analysis was conducted under the maximum-likelihood (ML) criterion with IQ-TREE version 2.22 (Minh *et al.* 2020), using the best fit model (K3Pu+F+G4) chosen by ModelFinder (Kalyaanamoorthy *et al.* 2017). Branch support was conducted using 1000 ultrafast bootstrap replicates (Hoang *et al.* 2018), with UFB ≥95 considered as robust. Two popular molecular species delimitation methods were used: (i) Assemble Species by

Automatic Partitioning (ASAP, Puillandre *et al.* 2021) was performed using the default setting using uncorrected p distance; and (ii) the Bayesian Poisson Tree Processes (bPTP, Zhang *et al.* 2013) was performed on the same data set using the default settings of 200,000 Markov chain Monte Carlo (MCMC) generations, thinning of 100, and 0.1 burn-in.

Results

Molecular Results

The final COI alignment consisted of 47 individuals of *P. quadridentatus*, and was 408 bp in length with 104 parsimony-informative sites. The phylogenetic reconstruction (Fig. 2) recovered a monophyletic *Pteromalus* that in our analyses included 13 named species. *Pteromalus quadridentatus* was retrieved as sister to *P. bedeguaris* (Thomson), a 3:4 mandibular formula species that is a parasitoid of rose gall wasps in Europe (Noyes 2019). These two species are sister to *P. puparum*, a widespread 4:4 mandibular formula species that is a parasitoid of various families of Lepidoptera. Another 3:4 mandibular formula species, *P. elatus* Förster, was sister to this clade, and the 4:4 species *P. apum* sister to that clade of four species. Consequently, our results do not support a monophyletic 4:4 mandibular formula clade, i.e. do not support a classification of *Pteromalus* that includes recognition of the subgenus *P.* (*Pteromalus*).

The species delimitation program ASAP recovered 12 putative species/molecular taxonomic operational units (MOTUs), matching all morphologically identified species with the exception of *P. albipennis* Walker/ *P. cingulipes* Walker being grouped as a single species (Fig. 2), which was previously discovered by Maletti *et al.* (2021). bPTP recovered all the same species as ASAP, but the five *P. apum* specimens were separated into individual MOTUs instead of grouping as one, for a total of 16 species.

Morphological Results

Species of *Pteromalus* with a 4:4 mandibular formula from regions other than North America where *A. rubi* is known. In addition to North America, *A. rubi* is recorded from western Europe and adjacent countries in North Africa (Algeria, Canary Islands) and western Eurasia (Armenia, Kazakhstan, Turkey) in the western Palaearctic. It is also recorded from the eastern Palaearctic (China: Hebei, Henan, Liaoning, Qinghai, Shandong, Shanxi; Russia: east Siberia; South Korea) and Oriental regions (China: Hubei, Sichuan) (Alonso-Zarazaga 2017; Anonymous 2021). Of these, because of trade, it is perhaps most likely that *A. rubi* was introduced from Europe or China.

Europe. Graham (1969) treated and keyed 67 named species of *Habrocytus* and *Pteromalus* from northwestern Europe. However, much remains to be done to resolve the taxonomy and, in particular, the correct nomenclature of European *Pteromalus*. Noyes (2019) listed about 375 species names of *Pteromalus* from Europe, with about 280 of these described by classical authors whose names have remained mostly unrecognized since their brief original descriptions. Graham (1969) treated eight species of *Pteromalus* with a 4:4 mandibular formula—*P. apum* (Retzius) [as *P. venustus* Walker], *P. bifoveolatus* Förster, *P. procerus* Graham, *P. proprius* Walker, *P. puparum* [type-species of *Pteromalus*], *P. smaragdus* Graham, *P. squamifer* Thomson, and *P. vopiscus* Walker. Using the key of Graham (1969) for *Pteromalus* females, those of our new species key readily to couplet 90 where *P. procerus* and *P. smaragdus* are differentiated. Among other features, *P. procerus* is eliminated as our new species because the male lacks a yellow-banded gaster and differs in other features given by Graham (1969) in the first half of couplet five of his key to males of the species. Males were not described for *P. smaragdus*, but females of our new species differ from described *P. smaragdus* females by the flagellum being entirely dark rather than conspicuously testaceous ventrally, the POL being at least 1.4× versus 1.15–1.2× the OOL, and the gaster being at least as long as (versus shorter than) the combined length of the head plus mesosoma. Using Graham's (1969) key to male *Pteromalus* the males of our new species key to couplet 40, regardless of whether in couplet 16 the flagellum is considered yellow or more or less brownish. Further, because of leg and antennal colour and a comparatively short postmarginal vein they key, with some difficulty, to couplet 43 where *P. dispar* (Curtis) and *H. hieracii* Thomson are differentiated. However, both of these species are characterized by a 3:4 mandibular formula.

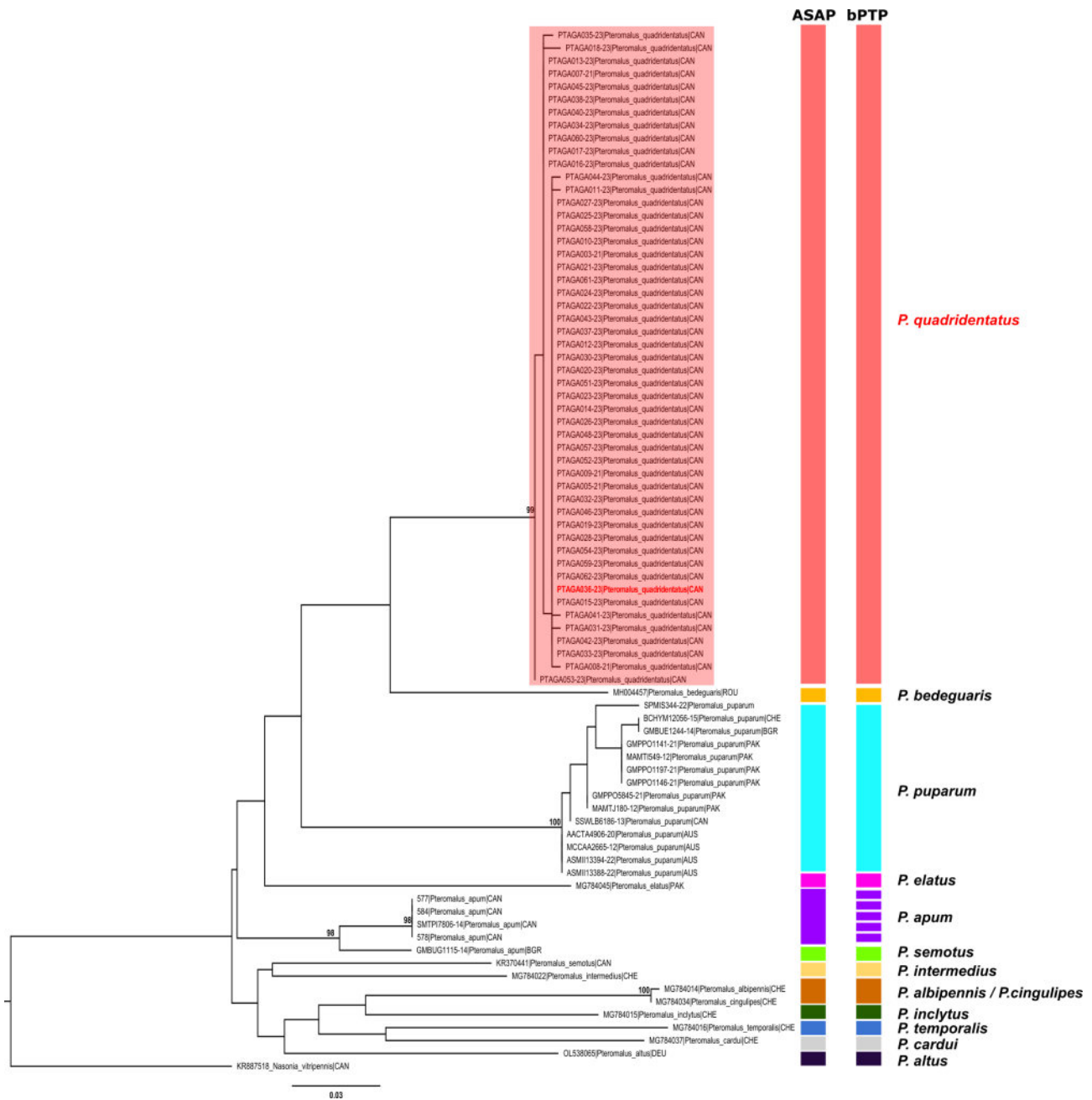


FIGURE 2. Phylogenetic tree and species delimitations recovered by programs ASAP and bPTP. The tree was inferred based on a Maximum Likelihood analysis with branch support estimated using 1000 ultrafast bootstrap replicates, with only values of >95 shown to indicate strong support. The monophyletic clade of *Pteromalus quadridentatus* is shaded pink and the holotype sequence in red font. The putative species recovered by ASAP and bPTP are represented by 12 different colour bars. The break in the purple coloured bars indicates that *P. apum* specimens were separated into five separate putative species based on the bPTP analysis. Codes next to specimen labels indicate the International Country Code where the specimen was collected, except for specimen SPMIS344-22 where the country of origin is unknown.

Since Graham (1969), six other species with a 4:4 mandibular formula have been described from Europe, but all are readily separated from our new species—*P. bottnicus* Vikberg (1979) from Finland [female flagellum paler (testaceous) ventrally, malar space at most half as long as eye, basal fold with 4–10 setae and 0–4 setae within basal cell apically], *P. briani* Baur (2015) from Switzerland [female legs yellow beyond coxae, male gaster dark], *P. discors* Graham (1992) from France [female antennal toruli distinctly closer to anterior ocellus than anterior margin of clypeus, marginal vein 1.1× length of stigmal vein, and postmarginal vein 1.4× as long as marginal vein], *P.*

osmiae Hedqvist (1979, fig. 2A) from Sweden [female basal cell completely setose, male gaster dark], *P. paludicola* Bouček (1972, figs 43, 45) from Czech Republic [female basal cell completely setose, flagellum with funiculars transverse, the apical funicular about 1.4× as broad as long, marginal vein only about 1.2× as long as stigmal vein], and *P. sylveni* Hedqvist (1979, figs 1C, 1F) [female clypeus deeply emarginate, malar space half height of eye, legs yellowish-red with all femora brown with tint of green on metafemur]. Consequently, no described species of *Pteromalus*, at least from northwestern Europe, is indicated as the species reared from *A. rubi* in Canada.

North Africa. Noyes (2019) reported just a single European species of *Pteromalus*, *P. puparum*, from Algeria, but 10 species from Canary Islands. Of the latter, five are European species treated by Graham (1969)—*P. albipennis*, *P. puparum*, *P. semotus* (Walker), *P. sequester* Walker, and *P. vibulenus* (Walker). Of the other five species, *P. canairensis* Janzon (1977) and *P. ellisorum* Gijswijt (1984) were described originally from Canary Islands. *Pteromalus canairensis* was described in *Habrocytus* and as belonging to the *sequester* group, and thus the mandibular dentition is almost certainly 3:4 even though this was not described. Regardless, females are differentiated by several features, including the speculum extending to the base of the stigmal vein, flagellum with quadrangular to transverse funiculars, and a short propodeum (Janzon 1977, figs B–D). *Pteromalus ellisorum* is also not our new species based on, among other features, males having the oral fossa reaching the ventral margin of the eye (Gijswijt 1984, fig. 2). The other three species, *P. amage* (Walker), *P. poisoensis* Graham, and *P. speculifer* Graham were all described from the island of Madeira, with both *P. poisoensis* and *P. speculifer* described in the subgenus *Habrocytus*, and thus with a 3:4 mandibular formula. Koponen and Askew (2002) treated *P. amage* from Madeira and stated that it is closely related to *P. platyphilus* Walker, a species also characterized by a 3:4 mandibular formula (Graham 1969).

Western Asia. Noyes (2019) recorded no species of *Pteromalus* from Armenia, whereas Rahmani *et al.* (2022) cataloged 12 species of *Pteromalus* from Turkey, but all are European species treated by Graham (1969). Dzhanokmen (1998) treated five species of *Pteromalus* from Kazakhstan with a 4:4 mandibular formula under *P. (Pteromalus)*. Of these, two are European, *P. bifoveolatus* and *P. puparum*, and the other three treated species, all parasitoids of Lepidoptera, were described as new—*P. melitaeae*, *P. maculatus*, and *P. transiliensis* Dzhanokmen. Of these, *P. transiliensis* was based only on females, who were described as having the fore wing basal cell extensively setose, whereas both *P. melitaeae* and *P. maculatus* were described from both sexes, the males of which were described as lacking a yellow spot on the gaster, and thus not our new species.

China. Noyes (2019) listed 12 species of *Pteromalus* from China, of which five are European species treated by Graham (1969)—*P. altus* (Walker), *P. bifoveolatus*, *P. procerus*, *P. puparum*, and *P. semotus*. The other seven species were described originally from China, of which *P. astragali* (Liao) in Liao *et al.* (1987), *P. coleophorae* Yang and Yao in Yang *et al.* (2015), *P. shanxiensis* Huang in Huang *et al.* (1987) and *P. xizangensis* (Liao) (1982) were all explicitly described as having a 3:4 mandibular formula or (*P. astragali*) described in *Habrocytus*. The mandibular formula of *P. miyunensis* Yao and Yang (2008) was not described, but the lateral habitus of the female in Yang *et al.* (2015, fig. 19) shows the legs to be yellowish beyond the coxae. *Pteromalus orgyiae* Yang and Yao in Yang *et al.* (2015) was described with a 4:4 mandibular formula, but the lateral habitus of the female in Yang *et al.* (2015) shows the legs to be comparatively pale beyond the coxae, and the fore wing basal cell and basal fold were described as setose. Finally, *P. qinghaiensis* Liao in Liao *et al.* (1987) was also described with a 4:4 mandibular formula, but the basal cell was described and illustrated as entirely setose except basally (Liao *et al.* 1987, pl. 57, fig. 2) and the scape described as dark rufous. Consequently, our new species also does not appear to be conspecific with any named *Pteromalus* species recorded from China.

Korea and east Siberia. Noyes (2019) recorded only a single species of *Pteromalus* from South Korea, *P. puparum*, whereas Tselikh (2020) reported four species, all with a 3:4 mandibular formula, from Eastern Siberia—*P. albipennis*, *P. berylli* Walker, *P. cardui* (Erdös), and *P. sequester*.

Species of *Pteromalus* with a 4:4 mandibular formula in North America north of Mexico. Noyes (2019) listed 39 valid, extant species of *Pteromalus* from the Nearctic region, of which only three, *P. anthonomi* (Ashmead), *P. obscuripes* (Ashmead) and *P. piercei* (Crawford) have been recorded as parasitoids of *Anthonomus* species. *Pteromalus piercei* was described originally with a 3:4 mandibular formula and this was stated also for *P. anthonomi* by Girault (1917). Girault (1917, p. 182) stated that the mandibles of *P. obscuripes* were tridentate and that the species “does not belong here” [*Habrocytus* ?]. Eighteen other recorded Nearctic species are also indicated to have a 3:4 mandibular formula based on their original description and/or treatment in Girault (1917) or Graham (1969)—*P. aulacis* (Girault), *P. bedequaris* (Thomson), *P. borrowi* (Girault), *P. canadensis* (Ashmead), *P.*

cerealellae (Ashmead), *P. damo* Walker, *P. egregius* Förster, *P. elevatus* (Walker), *P. epicles* Walker, *P. franciscanus* (Girault), *P. grisselli* Gibson, *P. lividus* (Gahan), *P. microps* (Graham), *P. onerati* Fitch, *P. phycidis* (Ashmead), *P. quinquefasciatus* (Girault), *P. rosae* (Girault), and *P. sequester*. *Pteromalus cyniphidis* (L.) is further assumed to have a 3:4 mandibular formula based on synonymy of *P. capreae* (L.) by Vikberg & Askew (2006), which was stated to have a 3:4 dentition by Graham (1969). *Pteromalus galliculus* Doğanlar (1980) was described as having four teeth on both mandibles, but examination of type material (CNC) clearly shows the left mandible has two ventral teeth and a dorsal truncation. The mandibular formula was not described and the left mandible is not visible in type material of 10 described species, but features are provided in the original descriptions or are visible in type material to exclude them as conspecific with our new species—*P. acutiventris* (Peck) [replacement name for *P. acutus* Provancher], *P. coeruleiventris* (Ashmead), *P. euryymi* Gahan, and *P. purpureiventris* (Ashmead) (female legs yellow), *P. americanus* (Girault) (costal setal line interrupted and speculum open at least to base of stigmal vein), *P. britanicus* (Girault) (female fore wing with triangular infuscate region near marginal and stigma veins), *P. coloradensis* (Ashmead) (costal setal line interrupted and propodeum similar to *P. elevatus*), *P. doryssus* Walker and *P. euthymus* Walker (males with femora and gaster dark), and *P. thyridopterigis* (Howard) (basal fold densely setose). Original descriptions are insufficient to exclude two species described by Provancher (1881) in *Habrocytus*, *P. fuscipes* and *P. melanicus*, as our new species and we did not personally examine type material. However, both were described from eastern Canada (Quebec) and a lateral image of the female lectotype of both (along with one for *P. acutiventris*) were provided to us by Joseph Moisan-De Serres. The lectotype of *P. fuscipes* has more oblong funiculars (Fig. 3A: insets) and paler brown femora (Fig. 3A) than females of our new species. *Pteromalus melanicus* was described from a single male and female. Unfortunately, the male syntype could not be located (Joseph Moisan-De Serres, personal communication), but the lateral image of the female lectotype also shows more oblong funiculars and a brighter metallic colouration (Fig. 3B) than our new species, and what appears to be a costal cell that is bare basally. The remaining four regional species, *P. apum*, *P. cassotis*, *P. hemileucae* and *P. puparum*, are known to have a 4:4 mandibular formula but are differentiated from our new species below.

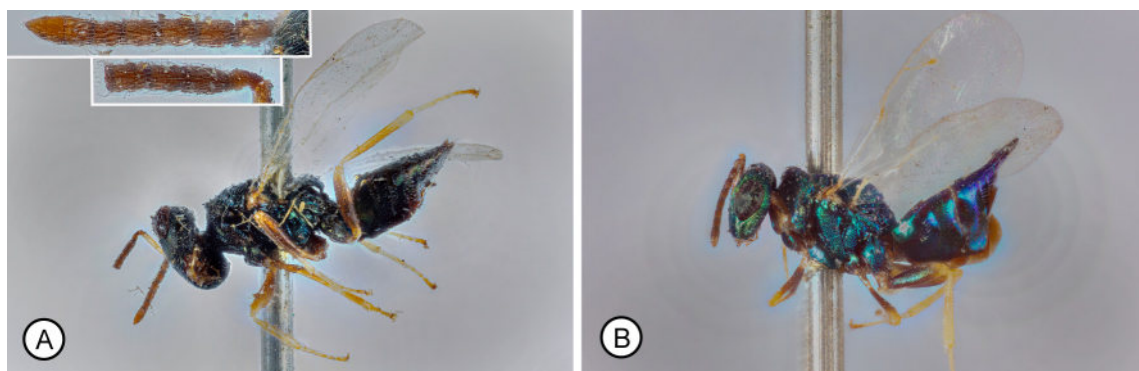


FIGURE 3. *Pteromalus* spp. (♀ lectotype), lateral habitus. **A**, *Pteromalus fuscipes* (insets; enlargement of antennae); **B**, *Pteromalus melanicus*.

Taxonomic treatment

Species of *Pteromalus* with a 4:4 mandibular formula in the Nearctic region

Diagnosis. Mandibles with 4 teeth (Fig. 4B). Female with following: clypeus with apical margin shallowly incurved or forming a broadly obtuse angle (Fig. 4B), and striate to strigose (Fig. 4B) or at most meshlike-reticulate basomedially (Fig. 5F); fore wing costal cell with ventral setal line entire, not interrupted medially (*cf.* Fig. 4D); fore wing disc uniformly setose behind marginal vein over at least apical half so as to obscure ventral setae, with setae along posterior margin of speculum abruptly angled toward marginal vein such that speculum more or less truncate apically (Figs 5H, 7E, 8E,G, 10H, 11H, 13D,H); propodeum with complete, sinuate, posteriorly subparallel plicae (Fig. 14D: pl) differentiating lateral panels (Fig. 14D: lp) and convex nucha (Fig. 14D: nu) from lateral collar region (14D: cr), with median length of lateral panels at least about one-third median length of scutellum and usually uniformly meshlike reticulate (Fig. 4F) though sometimes appearing partly, obliquely to horizontally strigose if

ridges of some cells aligned (Figs 11F, 14D), with nucha **usually** similarly meshlike reticulate as lateral panels (Fig. 4F), and with nuchal furrow (Fig. 14D: nuf) lacking longitudinal crenulae or at most with a single median carina and one additional carina on either side within furrow.

Remarks. The dentition of the left mandible (Fig. 4A,B) must be visible to reliably identify *Pteromalus* species with a 4:4 mandibular formula. However, if the mandibles are closed and the dentition is not visible, the females of many species with only three teeth on the left mandible (Fig. 4A) can be excluded based on one or more of the following features: apical margin of clypeus either straight-transverse or deeply and narrowly incised (bidentate); fore wing costal cell ventrally with setal line present only apically or obviously interrupted medially (Fig. 4C); fore wing disc dorsally bare behind marginal vein at least to base of stigmal vein (Fig. 4C) or setae forming posterior margin of speculum in virtually straight, oblique line toward marginal vein (sometimes with one to several setae in speculum apically or with single line of setae behind marginal vein within speculum, but these not obscuring ventral setae, Fig. 4D); propodeum otherwise structured or sculptured—lateral panels with median length obviously shorter than one-third length of scutellum and/or otherwise sculptured than meshlike reticulate, posteriorly with transverse adpetiolar strip (anteriorly angulate, transverse-triangular region) rather than convex, transverse-quadrangular nucha, or if with a convex nucha then this obviously sculptured differently from meshlike reticulate lateral panels (Fig. 4E) or nuchal furrow more extensively and regularly longitudinally crenulate.

Although some 3:4 species possess the same clypeal and fore wing setal features as 4:4 species, when different these features usually are sufficiently obvious to differentiate 3:4 from 4:4 species. Some 3:4 species also have very similar propodeal structure and sculpture features as 4:4 species and propodeal differences, particularly nuchal sculpture, can be less reliable for recognizing species of the two groups (see Remarks for *P. apum*).

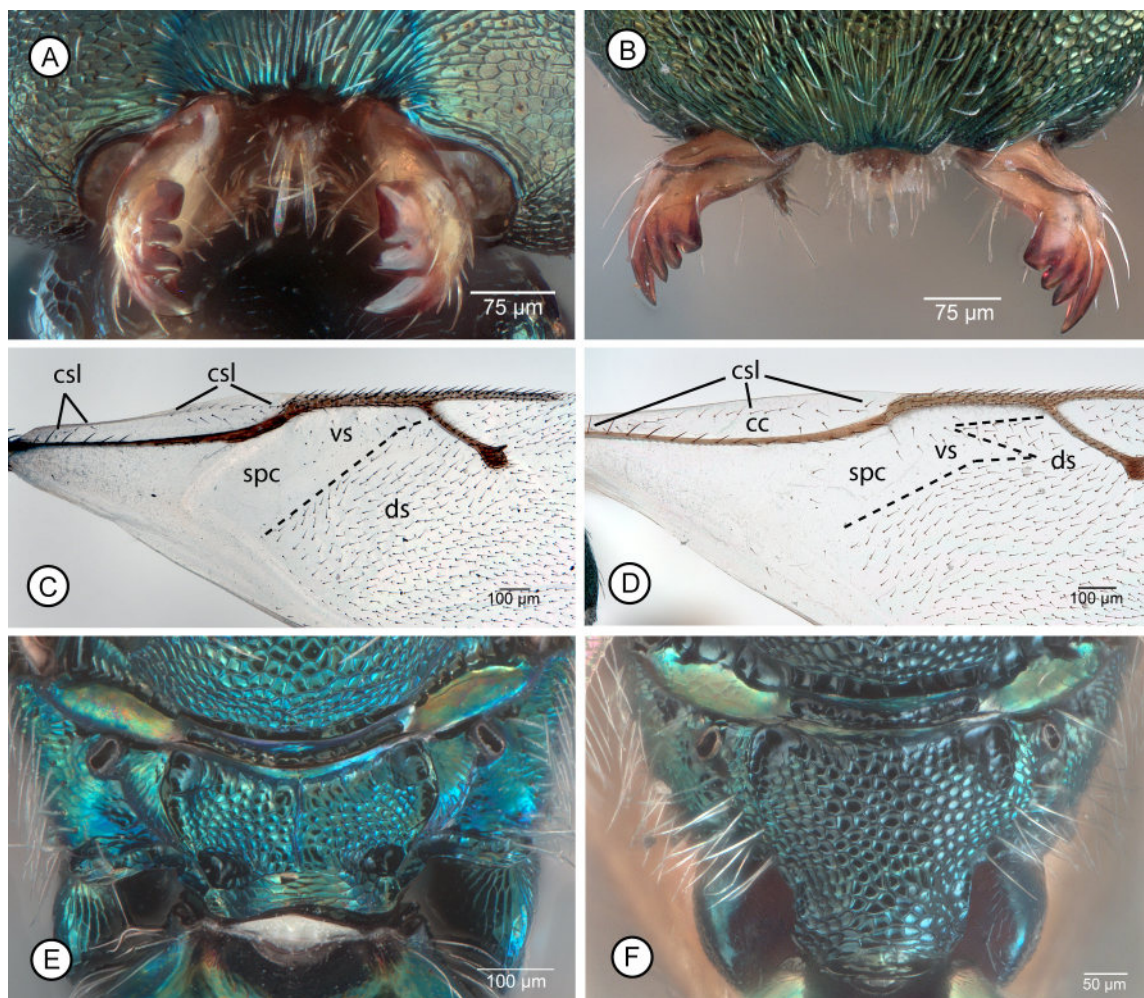


FIGURE 4. *Pteromalus* spp. (♀). **A–B**, labrum and mandibles: **A**, *Pteromalus semotus*; **B**, *Pteromalus quadridentatus*. **C–D**, basal half of fore wing: **C**, *P. sequester*; **D**, *P. semotus*. **E–F**, propodeum: **E**, *Pteromalus* sp. (*albibennis* species group); **F**, *P. cassotis*. See “Methods” for explanation of abbreviations; dashed lines on fore wings delineate basal limit of dorsal discal setae.

Key to species of *Pteromalus* with a 4:4 mandibular formula in the Nearctic region

- 1 Female 2
- Male 6
- 2(1) POL at least about 1.4× OOL (Figs 10C, 15A); fore wing basally bare or usually with only 1–3 dorsal setae on basal fold (Fig. 13D), though rarely with up to 6 dorsal setae including 1 seta either on mediocubital fold or within basal cell apically (Fig. 13H), **and** legs with at least basal three-quarters of all femora brown to black (Figs 10A, 13A,B) 3
- POL at most 1.2× OOL (Figs 5C, 7F, 11C); fore wing basally with basal fold and sometimes basal cell apically more extensively setose (Figs 7E, 8G, 11H) **or** legs paler, more or less uniformly yellowish to orange or with femora only somewhat darker reddish-brown (Fig. 8A,B) 4
- 3(2) Marginal vein at least 1.4× and usually about 1.5× longer than stigmal vein such that inner length longer than stigmal vein, and postmarginal vein at most as long as marginal vein (Fig. 13C); solitary parasitoid of Curculionidae *P. quadridentatus* Gibson n. sp.
- Marginal vein at most about 1.25× length of stigmal vein such that inner length appears at most about as long as stigmal vein, and postmarginal vein about 1.3× longer than marginal vein (Fig. 10H); gregarious parasitoid of Lepidoptera *P. hemileucae* Gahan
- 4(3) Scape extending dorsally only to about ventral margin of anterior ocellus (Fig. 5A,D) and antenna with funiculars beyond ful quadrangular to slightly transverse (Fig. 5G) such that combined length of flagellum and pedicel obviously less than width of head; legs with all femora dark to apices and metatibia mesally similarly dark as metafemur (Fig. 5A); fore wing with marginal vein, or at least inner length of marginal vein, subequal in length to stigmal vein (Fig. 5H) *P. apum* (Retzius)
- Scape extending dorsally above dorsal level of anterior ocellus to about level of vertex (Figs 7D, 8F, 11A) and/or antenna with most funiculars, including ful, usually obviously longer than wide (Figs 8F, 11G) such that combined length of flagellum and pedicel only slightly less than width of head; legs, or at least tibiae, sometimes extensively pale (Fig. 8A,C); fore wing with marginal vein sometimes obviously longer than stigmal vein 5
- 5(4) Legs with femora often with obscure metallic luster under some angles of light but at least variably dark brown, at least within basal half, compared to paler tibiae (Fig. 11A) (important to examine all three legs) *P. puparum* (L.)
- Legs with femora and tibiae more or less similarly yellow to variably dark orange (Fig. 8A,C) *P. cassotis* Walker
- 6(1) Hind leg with metafemur variably dark brown, conspicuously darker than metatibia (Fig. 6A,B); scape short, extending dorsally only to about ventral margin of anterior ocellus (Fig. 6D); flagellum with funiculars quadrate to transverse apically (Fig. 6D); gaster dark (Fig. 6A,B) *P. apum* (Retzius)
- All legs usually similarly yellow beyond coxae (Figs 9A–D, 12A) or metafemur only somewhat darker yellowish-orange (Fig. 16B); scape extending dorsally above level of anterior ocellus (Figs 9F, 12D, 15D); flagellum with funiculars oblong, longer than wide (Figs 9F, 12G, 15F,G); gaster sometimes with conspicuous yellow band subbasally (Figs 9C,D, 16A,B) 7
- 7(6) Gaster uniformly dark (Fig. 12B) (indeterminate specimens will key both ways) 8
- Gaster with subbasal yellow to brown or bronze region dorsobasally (Figs 9A, 16C: arrow), dorsally and ventrally (Fig. 9B: arrow), or with complete encircling yellow band (Figs 9C,D, 16A,B) 9
- 8(7) Lower face lateral of clypeus toward malar space and dorsally to lower inner orbit obliquely strigose-reticulate to pustulate-imbricate or rugulose, with sculpture obviously different than isodiametric meshlike sculpture of parascrobal region (Fig. 15E); POL conspicuously longer than OOL, by at least 1.6× (Fig. 15A,C) *P. quadridentatus* Gibson n. sp. (atypical, gaster shrunken/shrivelled)
- Lower face immediately lateral of clypeus transversely to obliquely elongate-reticulate but above level of clypeus isodiametric meshlike reticulate similar to parascrobal region (Figs 9G, 12F); POL less than 1.5× OOL (Figs 9E, 12C) *P. puparum* (L.) and rare *P. cassotis* Walker
- 9(8) Lower face lateral of clypeus toward malar space and dorsally to lower inner orbit obliquely strigose-reticulate to pustulate-imbricate or rugulose, with sculpture obviously different than isodiametric meshlike sculpture of parascrobal region (Fig. 15E); POL conspicuously longer than OOL, by at least 1.6× (Fig. 15A,C); gaster usually with complete encircling yellow band subbasally (Fig. 16A,B) *P. quadridentatus* Gibson n. sp. (typical)
- Lower face immediately lateral of clypeus transversely to obliquely elongate-reticulate but above level of clypeus isodiametric meshlike reticulate similar to parascrobal region (Fig. 9G); POL less than 1.5× OOL (Fig. 9E); gaster usually mostly metallic green except for subbasal yellow to brown or bronze region dorsobasally or dorsally and ventrally (Fig. 9A,B: arrow), though possibly rarely extending as complete band around gaster (Fig. 9C,D) (see species treatment) *P. cassotis* Walker

Pteromalus apum (Retzius)

Figs 5, 6

Ichneumon apum Retzius, 1783: 69 (♀).

Diplolepis apum, Spinola, 1808: 211.

Pteromalus apum, Nees ab Esenbeck, 1834: 104.

Pteromalus venustus Walker, 1835: 494 (♀). Synonymy by Bouček & Graham, 1978: 299.

Pteromalus planiscuta Thomson, 1878: 155 (♀, ♂). Synonymy by Bouček & Graham, 1978: 299; synonymy with *P. venustus* by Graham, 1969: 491.

Diagnosis. FEMALE. Head with POL and OOL of similar length (POL at most about 1.2× as long as OOL) (Fig. 5C); lower face, excluding clypeus, mostly isodiametric meshlike reticulate similar to parascrobal region, though gena obliquely strigose immediately above oral margin laterad clypeus (Fig. 5F: arrow). Antenna with scape comparatively short, extending dorsally only to about level of ventral margin of anterior ocellus (Fig. 5A,D); flagellum with fu2 and subsequent funiculars quadrate to apically transverse (Fig. 5G) such that combined length of pedicel and flagellum distinctly less than (at most about 0.8× as long) width of head. Fore wing basally (Fig. 5H) with at least 3 and usually more setae on basal fold, including sometimes apically on mediocubital fold and/or with 1 or 2 setae in basal cell apically; marginal vein similar in length to stigmal vein (at most about 1.2× as long, with inner length equal to or less than that of stigmal vein), and shorter than postmarginal vein. Legs with trochanters and trochantelli dark, similar to coxae and femora, all femora dark to apices, and meso- and metatibiae mesally similarly as dark as femora (Fig. 5A).

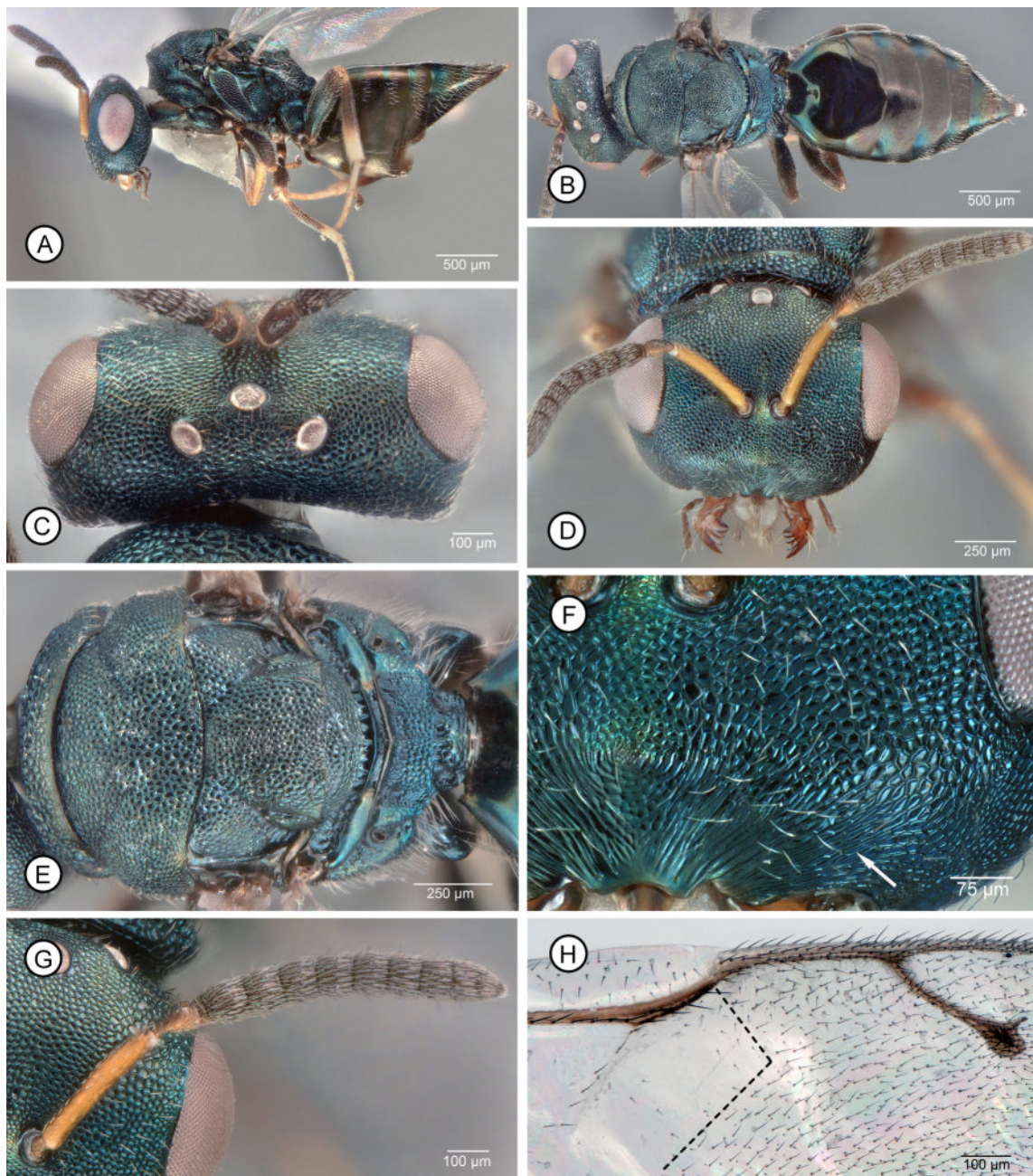


FIGURE 5. *Pteromalus apum* (♀). **A**, lateral habitus; **B**, dorsal habitus; **C**, head, dorsal; **D**, head, frontal and antennae; **E**, mesosoma, dorsal; **F**, lower face, frontolateral (arrow points to obliquely aligned sculpture); **G**, antenna; **H**, anteromedian part of fore wing (dashed lines delineate basal limit of dorsal discal setae).

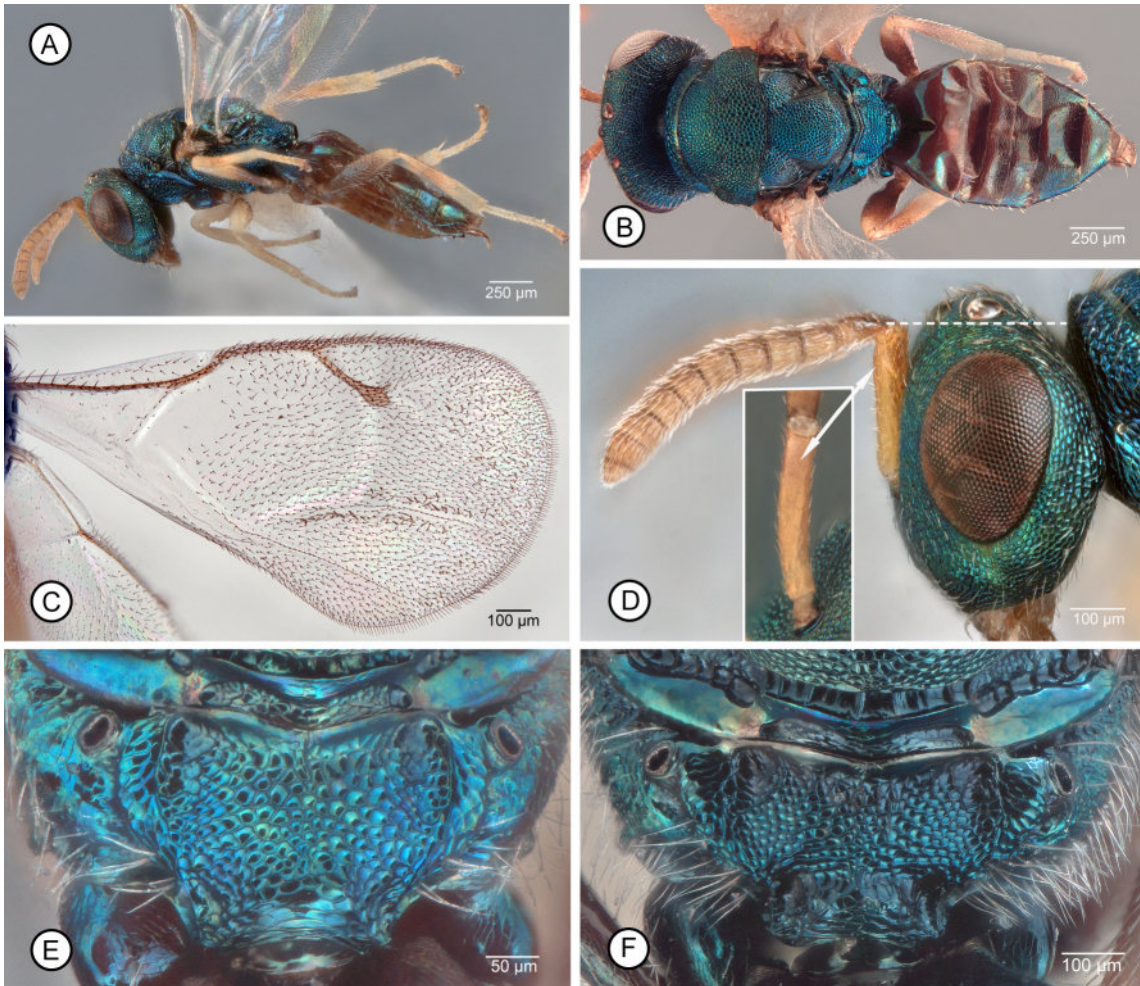


FIGURE 6. *Pteromalus apum*. A–E (♂): A, lateral habitus; B, dorsal habitus; C, fore wing; D, head and antenna, lateral (inset: ventral surface of scape) (horizontal dashed line indicates dorsal limit of scape relative to anterior ocellus, and arrow points to ventroapical smooth, setose region of scape); E, propodeum. F, propodeum (♀).

MALE. Head with POL: LOL and sculpture of lower face similar to that described for female. Antenna (Fig. 6D) yellow or pedicel brown dorsally and flagellum brownish-yellow; scape smooth and bare ventroapically (Fig. 6D inset: arrow), but without convex boss; relative dimensions of scape and flagellum similar to female, the funiculars quadrate to slightly transverse apically (Fig. 6D). Fore wing (Fig. 6C) similar to that described for female except basal cell sometimes with more setae. Front and middle legs entirely yellow or femora with basal half or less brown, but metafemur extensively brown except apically (Fig. 6A,B). Gaster entirely dark (Fig. 6A,B).

Molecular characterization. The average nucleotide composition of *P. apum* COI sequences is A = 42.0%, T = 32.3%, C = 12.3%, and G = 13.5%. All five *P. apum* sequences (Fig. 2) showed a high sequence identity, ranging from 99.26 to 99.46% identical.

Distribution. Nearctic, Neotropical and Palaearctic (see Noyes 2019).

Biology. Recorded primarily as a gregarious parasitoid of leafcutter bees (Megachilidae: *Megachile* spp.), but also of the honey bee (*Apis mellifera* L.), and of Erebidae (Arctiinae), Nymphalidae and Pieridae (Lepidoptera), plus a single record from *Oscinella frit* (L.) (Diptera: Chloropidae) (see references in Noyes 2019).

Remarks. Both Graham (1969) and Askew & Shaw (1997) remarked on the variability of *P. apum* females, particularly in the proportions of the funicular segments. Askew & Shaw (1997) also commented on perceived variation in relative length of the scape for females reared from lepidopteran hosts. Females they reared from some lepidopteran hosts had the scape extending dorsally to the middle or even the top of the anterior ocellus, though not females reared from *Megachile* species. Further, some females reared from *Gonepteryx rhamni* (L.) (Pieridae) had the marginal vein 1.35× the length of the stigmal vein, which is also the maximum length reported by Graham

(1969). However, individuals reared from *Megachile* and from other lepidopteran hosts had the marginal vein only about $1.0\text{--}1.1\times$ the length of the stigmal vein. The diagnosis presented herein for *P. apum* and illustrating macrophotographs are based only on CNC specimens reared from *Megachile rotundata* (Fabricius).

Among what we identify as *P. apum*, both sexes have comparatively more variable propodeal sculpture than the other treated 4:4 species. Different individuals have the plicae varying from abruptly differentiated ridges to being only slightly convex (Fig. 6F), and the reticulations of the nucha sometimes are quite obviously shallower compared to on the lateral panels and/or more transverse so as to appear more meshlike coriaceous (Fig. 6F) or transversely strigose (Fig. 6E).

Two females were borrowed from CBG and confirmed morphologically as *P. apum*: BIOUG15622-52 (BOLD id.: GMBUG1115-14) and BIOUG16060-101 (BOLD id.: SMT117806-14).

Pteromalus cassotis Walker

Figs 4F, 7–9

Pteromalus cassotis Walker, 1847: 393 (♀).

Pteromalus archippi Howard, 1889: 1891 (♀). *Synonymy* by Burks, 1975: 154.

Diagnosis. FEMALE. Head with POL and OOL of similar length (POL less than $1.2\times$ OOL) (Fig. 7F); lower face, excluding clypeus, mostly similarly isodiametric meshlike reticulate as parascrobal region, though usually obliquely strigose immediately lateral of clypeus (Fig. 8H: arrow). Antenna with scape comparatively long, extending dorsally almost to level of vertex (Figs 7D, 8F); flagellum with basal funiculars oblong, longer than wide, and apical funiculars quadrangular to slightly longer than wide (Fig. 8F) such that combined length of pedicel and flagellum only slightly less than width of head. Fore wing (Fig. 8E) with basal fold and basal cell bare (Fig. 8E) or with uniformly spaced line of setae along basal fold and sometimes with some setae apically in basal cell (Fig. 7E: dorsal setae numbered, 8G); marginal vein about $1.3\text{--}1.4\times$ length of stigmal vein (Figs 7E, 8E) and of similar length or only slightly shorter than postmarginal vein. Legs usually uniformly yellow (Fig. 8A) to variably dark orange (Fig. 8C) beyond coxae or if femora slightly darker than tibiae then not brown.

MALE. Head with POL about $1.4\times$ OOL (Fig. 9E); lower face similar in sculpture to female, mostly meshlike reticulate as parascrobal region except for clypeus and immediately laterad clypeus (Fig. 9G). Antenna (Fig. 9F) yellow or pedicel brown dorsally and flagellum brownish-yellow; scape without ventroapical boss (Fig. 9F: inset); relative dimensions of scape and flagellum similar to female, the funiculars obviously oblong. Fore wing of typical form (Fig. 9H) with at least 6 setae along basal fold and with up to 14 setae basally including within basal cell and on mediocubital fold apically. Legs entirely yellow beyond coxae or sometimes somewhat darker, more orange (Fig. 9A–D). Gaster of typical form mostly dark but with variably large and distinct, yellow to bronze or non-metallic brown region subbasally both dorsally and ventrally (Fig. 9A,B: arrow) or rarely essentially uniformly dark (see Remarks).

Distribution. Nearctic (Noyes 2019; Stenoien *et al.* 2015).

Biology. A gregarious parasitoid of the pupae of Nymphalidae and Papilionidae (Lepidoptera) (Noyes 2019).

Remarks. Although not described originally, type images of the lectotype fore wing provided to us show what is likely seven dorsal setae along the basal fold and within the basal cell apically (Fig. 7E: setae numbered). Two additional horizontal dark lines near the parastigma in the speculum (Fig. 7E: vs) may be additional setae but, if so, likely are on the ventral rather than dorsal surface based of their horizontal rather than vertical orientation. The majority of females in the CNC that we identify as *P. cassotis* have more reduced basal fold/cell setation (Fig. 8E) than the lectotype (Fig. 7E), though some have setal patterns similar to the lectotype (Fig. 8G, see further below). Females we identify as *P. puparum* typically have several setae on the basal fold and apically in the basal cell (Fig. 11H) similar to the lectotype of *P. cassotis*, though some have only two or three setae on the basal fold, more similar to typical *P. cassotis* females. Provided images of the lectotype also show the fore wing disc has dorsal setae (vertical setae pointing toward the leading margin) behind the marginal vein for virtually its entire length, although more posteriorly the apical angle of the speculum extends behind about the basal half of the marginal vein (Fig. 7E: dashed lines). Further, the marginal vein is about $1.3\times$ the stigmal vein (Fig. 7E), the POL and OOL are of similar length, the POL only about $1.1\times$ the OOL (Fig. Fig. 7F), and the propodeum lacks a median carina (Fig. 7E). Baur (2015) differentiated *P. cassotis* from his new species *P. bryani* by several features, but only one feature differed

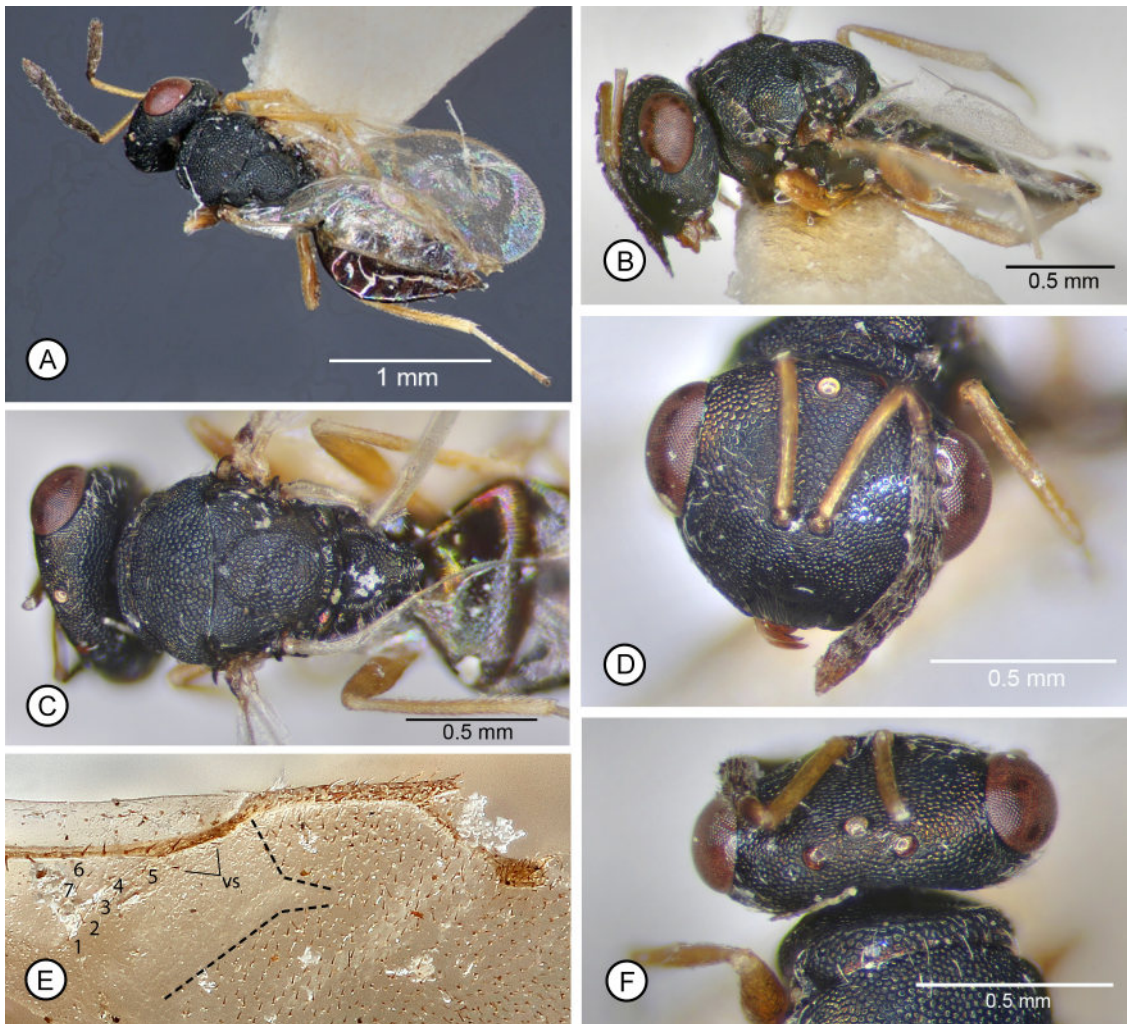


FIGURE 7. *Pteromalus cassotis* type material (♀). **A**, dorsal habitus (PT #5.754b); **B**, lateral habitus (PLT #5.74c); **C**, head and mesosoma, dorsal (PLT #5.74c); **D**, head, frontal (PLT #5.74c); **E**, anteromedian part of fore wing (LT) (numbers mark dorsal setae on basal fold and in basal cell; dashed lines delineate basal limit of dorsal discal setae; vs = ventral setae); **F**, head and pronotum, dorsal (PLT #5.74c). Abbreviations: LT = lectotype, PLT = paralectotype. Specimen images ©The Trustees of the Natural History Museum, London, available under Creative Commons License 4.0 (<https://creativecommons.org/licenses/by/4.0/>)

from those provided for *P. puparum*. The femora of female *P. puparum* were stated as “infuscate” (dark brown to blackish), whereas they were stated as “testaceous” (reddish-brown) for *P. cassotis* females. Our concept of *P. cassotis* includes females that typically have the legs more or less uniformly yellow to variably dark orange beyond the coxae. Walker (1847) described the legs for female *P. cassotis* as “fulvae” (brownish-yellow, orange) except for “flavi” (yellowish) meso- and metatarsi. Images of the lectotype and paralectotype provided to us show the left legs to be somewhat darker reddish-brown than the more yellowish right legs (Fig. 7A,C), which suggests that colour in the images is influenced by lighting or perhaps preservation state of the specimens. Regardless, the femora and tibiae of either side are similar in colour to each other (Fig. 7A,C). Typical females we identify as *P. puparum* have the femora darker, more distinctly brown to dark than the respective tibia (Fig. 11A). Some females we tentatively identify as *P. puparum* have comparatively pale femora, similar to *P. cassotis*, but mesally the femora are darker than the tibiae. In differentiating *P. cassotis* and *P. puparum* based on relative femora-tibiae colour pattern it is important to examine all three legs, not just the hind leg. Further, it remains to be proven through molecular analyses whether females with what appear to have intermediate leg colour patterns are *P. cassotis* or *P. puparum*, and the extent of variation in leg colour possible for both putative species.

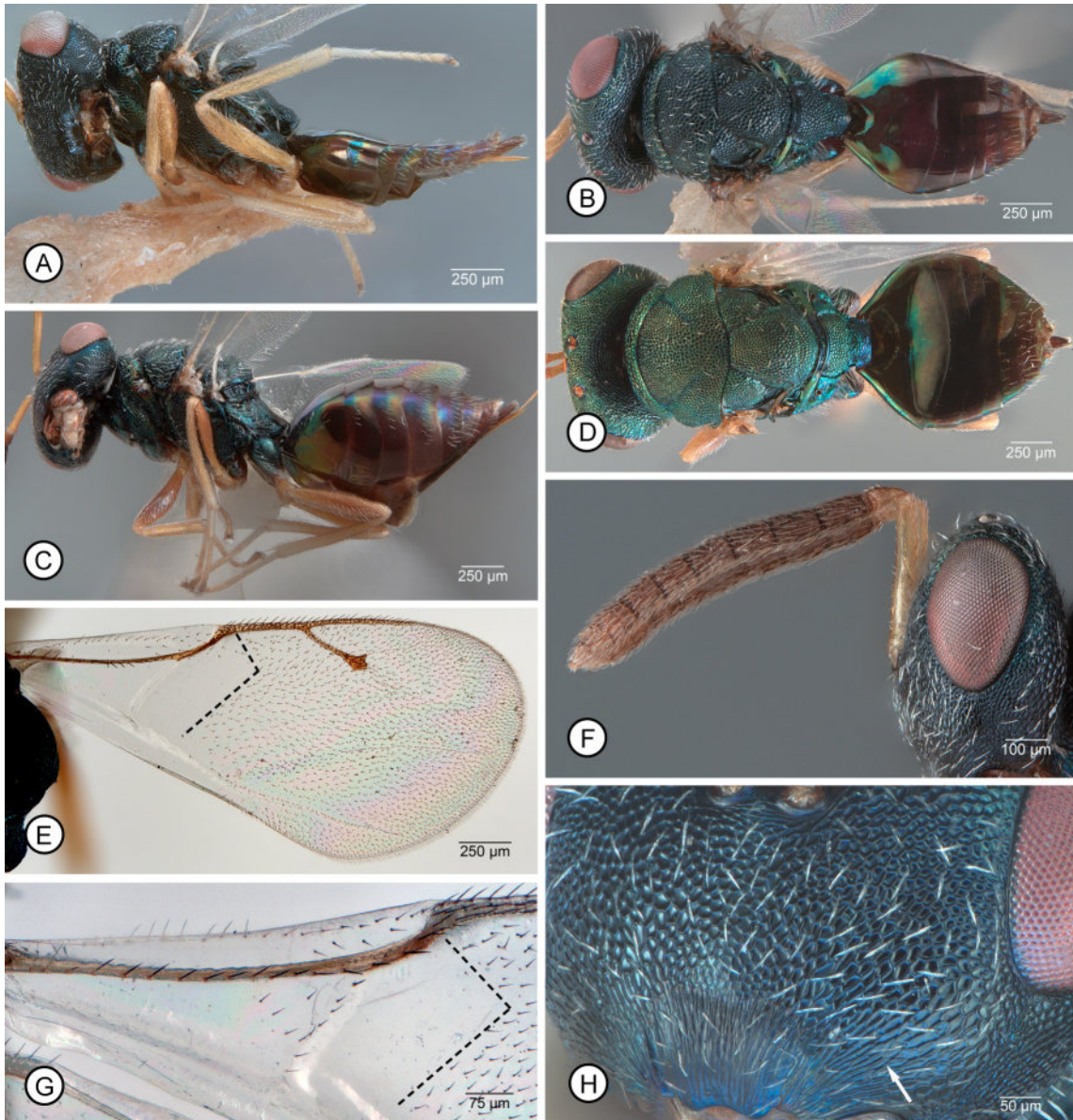


FIGURE 8. *Pteromalus cassotis* (♀). All images except A, C—E of specimens identified as *P. archippi* by B. Burks (see species treatment): **A**, lateral habitus; **B**, dorsal habitus; **F**, head and antenna, lateral **G**, basal part of fore wing; **H**, lower face, frontolateral (arrow points to obliquely aligned sculpture). **C**, lateral habitus of female with comparatively dark femora. **D–E**, Vernon, BC female (see species treatment): **D**, dorsal habitus; **E**, fore wing. Dashed lines on E and G delineate basal limit of dorsal discal setae.

Walker (1847) did not describe the male of *P. cassotis*. The CNC has three series of reared individuals consisting of both sexes that we identify confidently as *P. cassotis*. Two of the series were identified as *P. archippi* by O. Peck (formally CNC)—Windsor, Ontario, 24.VI.1953, Plant Prot. 5A, reared from “*Basilarchia archippus*” (2♀, 2♂), and Viellardville, Saskatchewan, 1967, J.C. Melvin, reared from “*Limenilus arthemis*” (2♀, 3♂). The USNM also has two series of reared individuals identified as *P. archippi* by A.B. Gahan (formally USNM)—Auburn, Alabama, 8.X.1942, J.T. Griffiths, reared from “cabbage worm” (1♀, 1♂), and Caney Spring, Tennessee, G.G. Ainslie (3♀, 2♂ + unidentified lepidopteran chrysalis under Webster No. 13891 and Knoxville No. 1650). Females of all four series are of the form having yellow legs and fore wings with setae along the basal fold and within the basal cell apically (Fig. 8G) or at least a complete line of setae along the basal fold. Associated males of each series have entirely yellow legs and antennae in combination with a gaster that has a variably large and distinct, subbasal yellow to non-metallic brown or bronze region that does not encircle the gaster (Fig. 9A,B: arrow). The third CNC series,

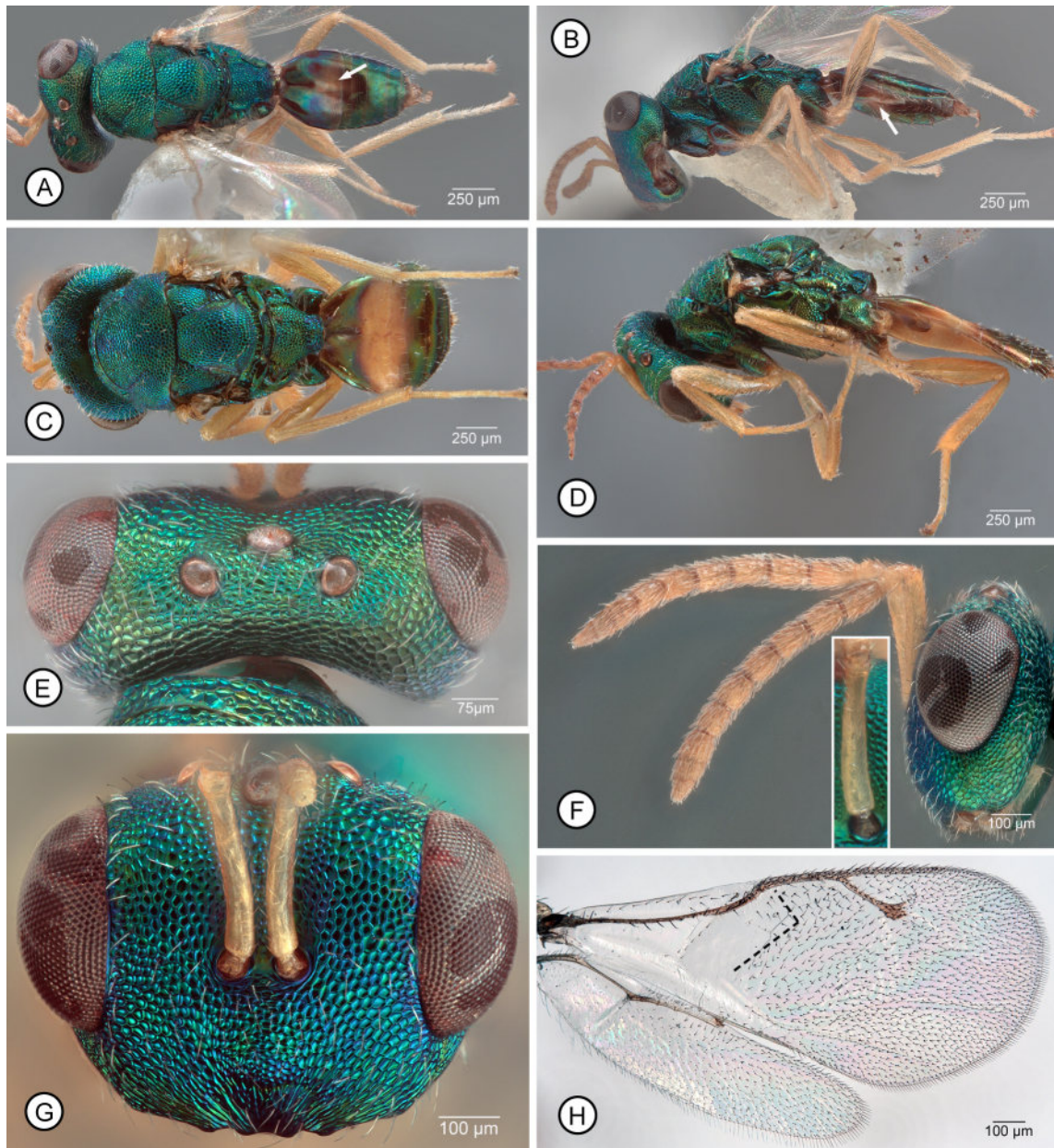


FIGURE 9. *Pteromalus cassotis* (♂). All images except C and D identified as *P. archippi* by B. Burks or O. Peck (see species treatment): A, dorsal habitus; B, lateral habitus; E, head, dorsal; F, head and antennae, lateral (inset: ventral surface of scape); G, head, frontal; H wings (dashed lines delineate basal limit of dorsal discal setae). C–D, Vernon, BC male: C, dorsal habitus; D, lateral habitus. Arrows on A and B point to paler subbasal region of gaster.

from London, Ontario, VII.1950, O. Peck (4♀, 4♂) is similar to the four series that were identified as *P. archippi*, but the males could be more readily misidentified as *P. puparum* because the basal paler region is the least developed, at best only obscurely evident in two of the males. In addition to these, the CNC has a reared series from Vernon, British Columbia, 2.III.1934, G.R. Hoping, labelled as “reared from chrysalis of *Papilio* sp.” (13♀, 5♂). The USNM has an additional eight females and one male labelled Northport, Washington, VI.1934, A. McCallum (handwritten label), emerged Vernon, B.C., 25.VI.1934, G.R. Hoping (same printed label as CNC specimens), host “*Aglais*” (= *Nymphalis*) “*californica* Bvd.”. The CNC and USNM series are thus apparently from the same rearing event. Females have yellowish to reddish-yellow legs beyond the coxae similar to the other series, but differ in having the fore wings entirely bare basal to the level of the marginal vein (Fig. 8E) and they have an almost subcircular gaster that is only slightly longer than wide and about 0.8× the length of the mesosoma (Fig. 8D). Typical females

we identify as *P. cassotis*, including some lacking setae basally on the fore wing, have a more distinctly lanceolate gaster that is somewhat longer than the mesosoma (Fig. 8A–C). Associated males of the series are also exceptional in having a broad yellowish band that fully encircles the gaster (Fig. 9C,D). These males are thus very similar in colour pattern to those of *P. quadridentatus*, but unlike the latter have the lower face lateral of the clypeus mostly similarly meshlike reticulate as the parascrobal region (Fig. 9G). Similar to their conspecific females the males have reduced fore wing setae basally compared to what we identify at typical *P. cassotis* males, having 0–3 setae on the basal fold compared to at least 6 setae along the basal fold and up to 14 setae along the basal fold and mediocubital fold and basal cell apically. The males are similar to males that were reared in Mexico from *Papilio (Pterourus) multicaudata* Kirby (Lepidoptera: Papilionidae) and identified as *P. puparum* by Jiménez-Galván *et al.* (2020). Females were not clearly imaged by Jiménez-Galván *et al.* (2020, fig. 1e), though they appear to have quite dark reddish-brown legs. Two different males were imaged, one laterally and one dorsally, and both clearly show a broad subbasal pale gastral band (Jiménez-Galván *et al.* 2020, fig. 1b, c). Facial sculpture is not visible in either the lateral or dorsal images of the two males, but in the dorsal image the POL is subequal in length to the OOL. Thus, the species cannot be *P. puparum* or *P. quadridentatus* but more likely is *P. cassotis* or some similar undescribed species, as may be the Northport/Vernon specimens.

Reared males of *P. quadridentatus* demonstrate that even though the gaster usually has a broad encircling yellowish band, this is sometimes reduced or very rarely the gaster appears essentially entirely dark when the gaster is shrivelled (Fig. 16C). Therefore, it is quite possible that gastral colour pattern also varies for male *P. cassotis*, possibly from essentially entirely dark to having a complete encircling pale band. Further, although the difference in leg colour described for female *P. cassotis* and *P. puparum* is usually quite obvious, some museum specimens are difficult to confidently assign to one or the other species by this feature alone, particularly because fore wing basal fold/cell setal patterns also appear to overlap in the two species. Both species are gregarious parasitoids of Lepidoptera and comprehensive studies involving both molecular and morphological evidence are necessary to evaluate further the morphological limits of *P. cassotis*, including gastral shape for females, gastral colour pattern for males, and fore wing setal pattern for both sexes.

***Pteromalus hemileucae* Gahan**

Fig. 10

Pteromalus hemileucae Gahan, 1917: 210–211 (♀).

Diagnosis. FEMALE. Head with POL about 1.4× OOL (Fig. 10C); lower face mostly isodiametric meshlike reticulate (Fig. 10D,F) lateral of clypeus to and below lower orbit, though sculpture finer, more imbricate-reticulate near oral margin. Antenna (Fig. 10G) with scape comparatively long, extending dorsally to about level of vertex; flagellum with basal funiculars oblong, distinctly longer than wide, but funiculars shorter apically such that apical funicular only slightly longer than wide and combined length of pedicel and flagellum subequal in width to head. Fore wing (Fig. 10H) with basal fold, basal cell and mediocubital fold bare or at most with 1 or 2 setae within basal cell; marginal vein at most about 1.25× length of stigmal vein (inner length at most as long as stigmal vein), and at most only about 0.8× length of obviously longer postmarginal vein. Legs (Fig. 10A,B) with all femora brown except apically and metatibia mostly pale but somewhat darker brownish subbasally.

MALE. Unknown.

Distribution. Nearctic (USA: New Mexico), Neotropical (Mexico).

Biology. Described originally as a gregarious parasitoid of a pupa of *Hemileuca oliviae* Cockerell (Lepidoptera: Saturniidae).

Remarks. Gahan (1917) described *P. hemileucae* based on 13 females reared from a single chrysalis. The USNM has the chrysalis and 11 females, of which one has a red label with “Type No. 20389” and databased as “USNMENT 01520630”, and the other 10 having red labels with “Paratype No. 20389”; however, all specimens are syntypes because Gahan did not designate a holotype in the publication and a lectotype has yet to be designated. All are dirty and variably extensively covered by glue or some other oily film (Fig. 10). Among other features, Gahan (1917, pp. 210–211) described the POL as distinctly longer than the OOL, the stigmal vein only slightly shorter than the marginal vein, the postmarginal vein much longer than the marginal, the flagellum nearly black, and all femora

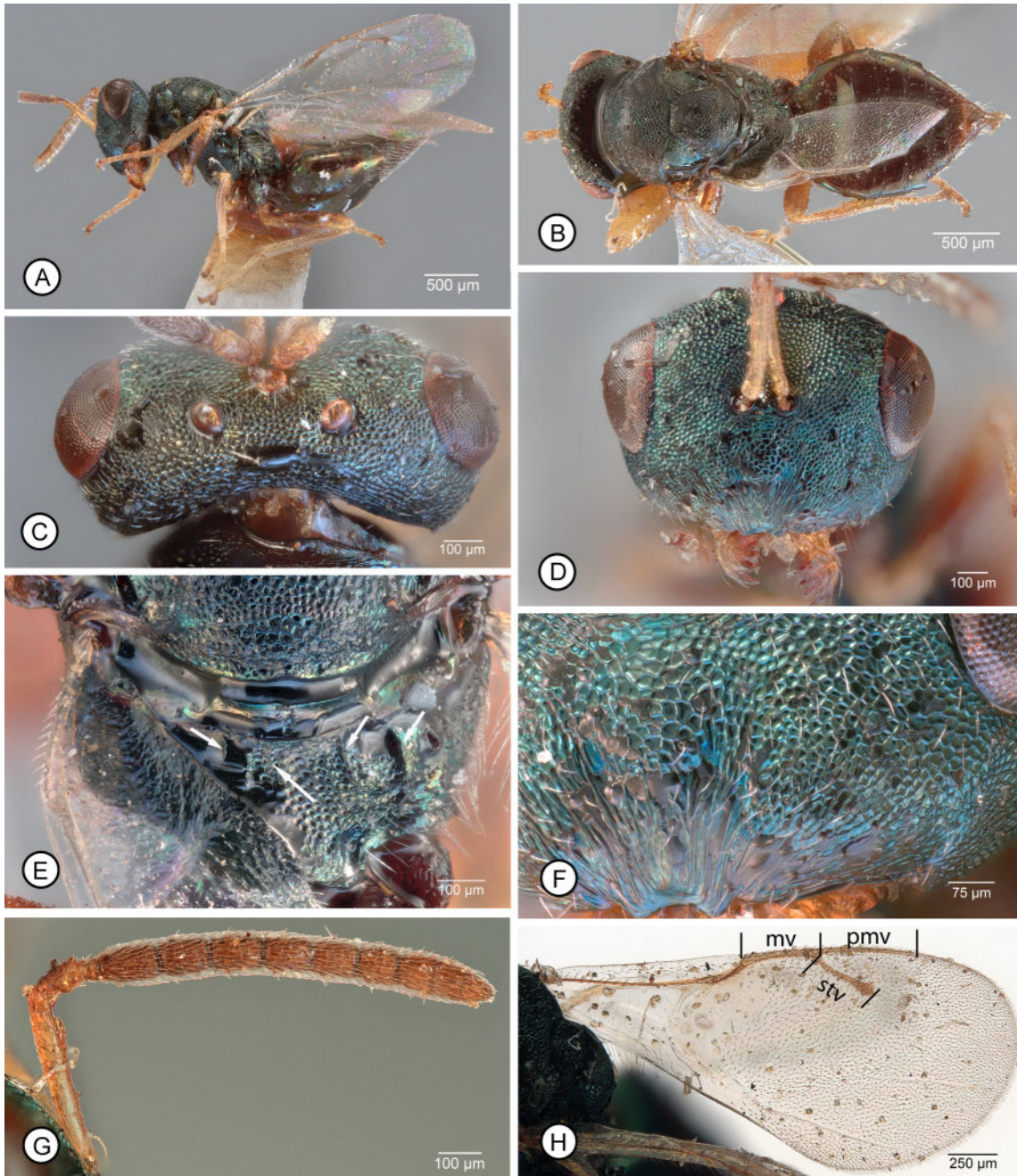


FIGURE 10. *Pteromalus hemileucae* (♀ syntypes). **A**, lateral habitus; **B**, dorsal habitus; **C**, head, dorsal; **D**, head, frontal; **E**, apex of scutellum to propodeum (arrows point to median carina and crenulae along anterior margin); **F**, lower face, frontolateral; **G**, antenna; **H**, fore wing. Abbreviations: mv = marginal vein, pmv = postmarginal vein, stv = stigmal vein.

dark brown with the basal half of the meso- and metatibia brownish. All of these features are confirmed by the type series except the flagellum is only somewhat darker brownish-yellow to pale brown compared to a yellowish scape (Fig. 10G) rather than being nearly black. Further, in the type specimens the postmarginal vein gradually tapers and fades apically so that its apical limit is difficult to discern accurately, but the postmarginal vein is at least obviously longer than the marginal vein (Fig. 10H). Freshly collected specimens are necessary to determine whether discrepancies between the description and the type specimens result from the specimens fading in the over 100 years since they were collected. Gahan also described the head and mesosoma as “dark greenish” (Fig. 10A–F) and stated that the propodeum lacks a median carina. All females have the propodeum at least partly obscured by the wings (Fig. 10E), but some have a median carina within the nuchal furrow that sometimes extends toward and almost joins

a carina (Fig. 10E: median arrow) within a row of comparatively long carinae anteriorly along the anterior margin of the propodeum (Fig. 10E: lateral arrows). In such females there is some indication of an obscurely developed median carina; in addition, some females have a carina within the nuchal furrow on either side of the median carina such that there are three carinae in the furrow between the plical carinae. Although not clearly measurable in any female, the plical region may be somewhat more transverse than for *P. quadridentatus* or at least at the upper end of variation for that species, i.e. about 1.5× wider than the median length of the propodeum. The type series females do have a more ovate gaster (Fig. 10B) than *P. quadridentatus* females (Fig. 13B,F), being at most only about 1.5× versus at least 1.8× as long as wide. Further, the sculpture of the lower face lateral to the supraclypeal area is more extensively isodiametric meshlike reticulate (Fig. 10D,F) than for *P. quadridentatus* females (Fig. 14 B,F), though this latter difference is more subtle.

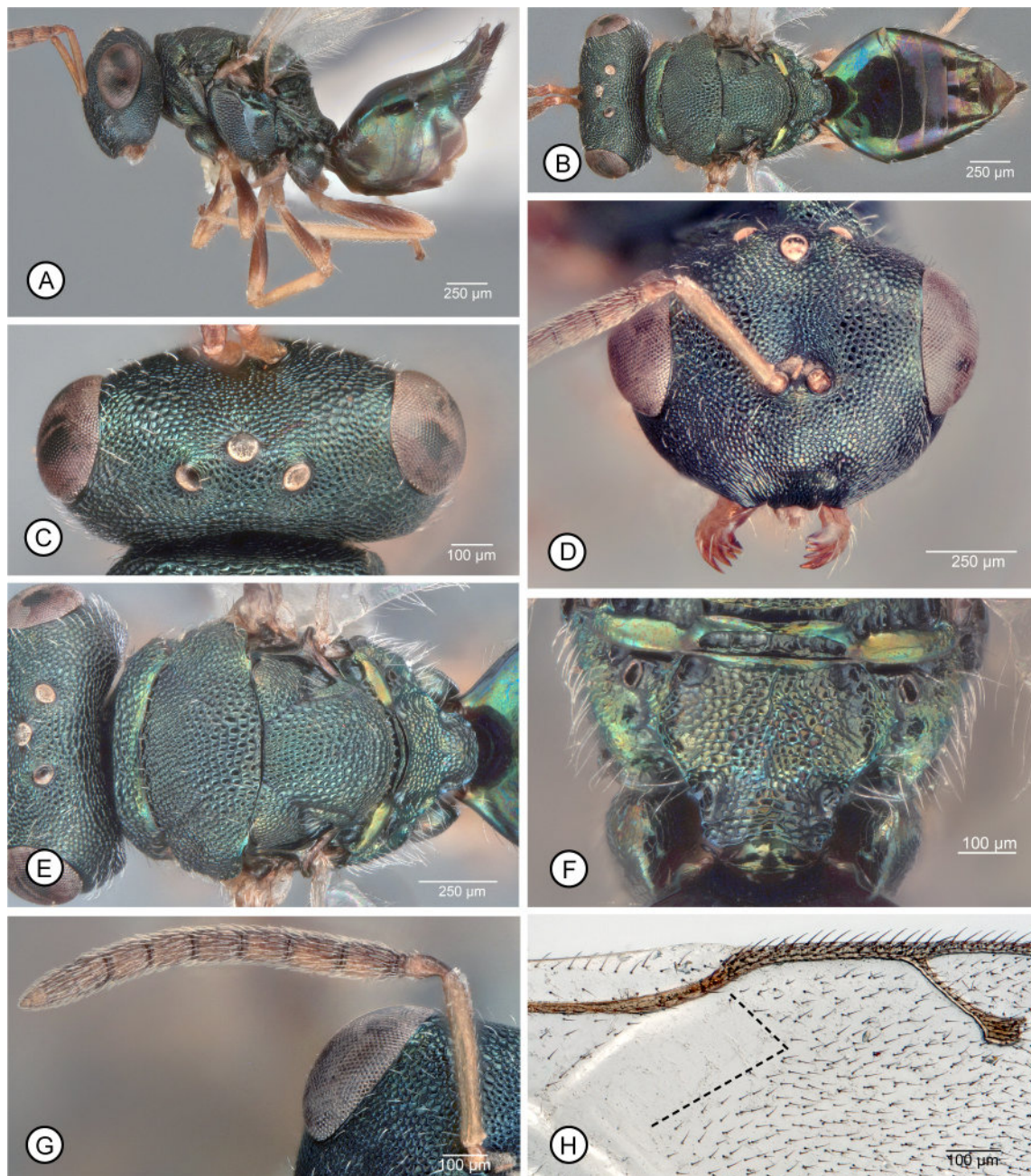


FIGURE 11. *Pteromalus puparum* (♀). **A**, lateral habitus; **B**, dorsal habitus; **C**, head, dorsal; **D**, head, frontal; **E**, vertex and mesosoma, dorsal, **F**, propodeum; **G**, antenna; **H**, anteromedian part of fore wing (dashed lines delineate basal limit of dorsal discal setae).

***Pteromalus puparum* (Linnaeus)**

Figs 11, 12

Ichneumon puparum, Linnaeus, 1758: 567 (♀).

Cynips puparum, Fourcroy, 1785: 387.

Cynipsichneumon puparum, Christ, 1791: 383.

Diplolepis puparum, Fabricius, 1804: 151–152.

Pteromalus puparum, Swederus, 1795: 203.

Chalcis puparum; Junine, 1807: 316.

Synonymy. In addition to the different generic concepts listed above, Noyes (2019) cited 17 junior synonyms of *P. puparum*, which reflects not only the 265 years since the species was first described, but also its cosmopolitan distribution.

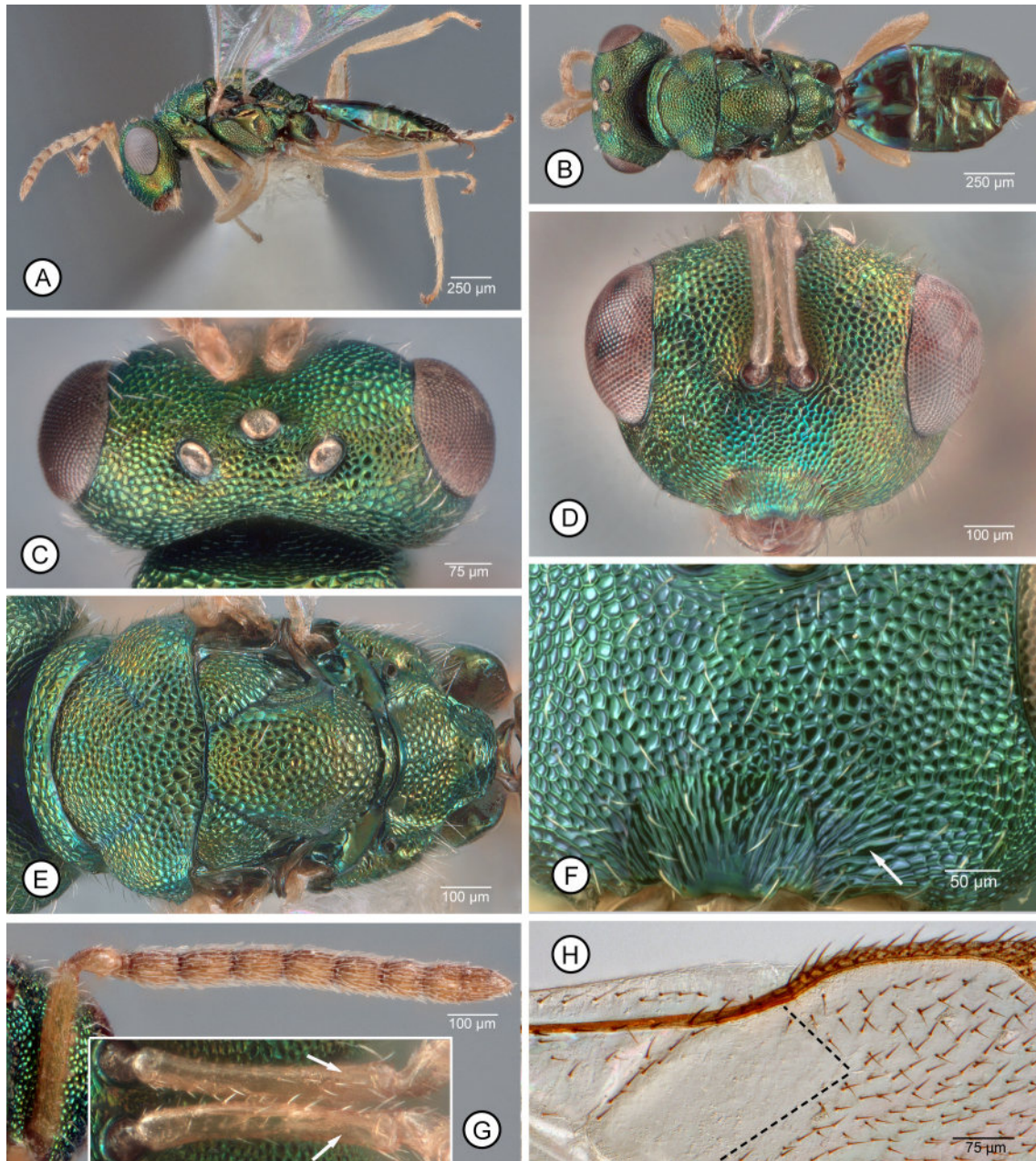


FIGURE 12. *Pteromalus puparum* (♂). **A**, lateral habitus; **B**, dorsal habitus; **C**, head, dorsal; **D**, head, frontal; **E**, mesosoma, dorsal; **F**, lower face, frontal; **G**, antenna (inset: scapes, ventral view, arrows point to smooth, setose ventroapical region); **H**, anteromedian part of fore wing (dashed lines delineate basal limit of dorsal discal setae).

Diagnosis. FEMALE. Head with POL and OOL of similar length (POL less than $1.2 \times$ OOL) (Fig. 11C); head with lower face obliquely strigose-reticulate lateral of clypeus to about level of base of clypeus but otherwise meshlike reticulate similar to parascrobal region (Fig. 11D). Antenna (Fig. 11G) with scape comparatively long, extending dorsally about to level of vertex (Fig. 11A); flagellum (Fig. 11G) with basal funiculars oblong, longer than wide, and apical funiculars quadrangular to slightly longer than wide such that combined length of pedicel and flagellum only slightly less than width of head. Fore wing with basal fold rarely with only 2 or 3 setae, but usually more extensively setose, including apically in basal cell (Fig. 11H); marginal vein about $1.3\text{--}1.4 \times$ length of stigmal vein and of similar length to or only slightly shorter than postmarginal vein. Legs (Fig. 11A) usually with femora black, sometimes with slight metallic luster, but if paler, variably dark brown, then obviously darker than obviously paler, brownish-yellow to yellow tibiae.

MALE. Head with POL: OOL (Fig. 12C) similar to female; lower face sculpture (Fig. 12F) similar to female, meshlike reticulate similar to parascrobal region except for clypeus and immediately lateral of clypeus. Antenna (Fig. 12G) yellow or pedicel brown dorsally and flagellum brownish-yellow, scape smooth and bare ventroapically (Fig. 12G: inset), but without convex boss; relative dimensions of scape and flagellum similar to female, the funiculars obviously oblong. Fore wing setal pattern (Fig. 12H) and relative length of venation similar to those described for female, though basal fold usually with complete line of setae. Legs entirely yellow beyond coxae or sometimes somewhat darker, more orange (Fig. 12A,B). Gaster entirely dark (Fig. 12A,B).

Molecular characterization. The average nucleotide composition of *P. puparum* COI sequences is A = 33.5%, T = 38.8%, C = 15.1%, and G = 12.6%. The 14 *P. puparum* sequences (Fig. 2) ranged from 98.05 to 100% identical.

Distribution. Cosmopolitan, Noyes (2019) listed over 60 countries from all biogeographic realms.

Biology. Mostly recorded as a primary gregarious parasitoid of the pupae of 17 different families of Lepidoptera, but Noyes (2019) also included host records for Coleoptera (Bruchidae, Curculionidae and Scolytidae), Diptera (Chloropidae), Hemiptera (Diaspididae) and Hymenoptera (Cynipidae, Sphecidae, Vespidae). Noyes (2019) also reported instances of hyperparasitism through Pteromalidae and Ichneumonoidea.

Remarks. The uncertainty in the extent of leg colour variability and fore wing setal pattern, and issues of confidently differentiating museum specimens of *P. puparum* from *P. cassotis*, are discussed under the latter species. In addition to antennal features, hind leg colour pattern is also useful for differentiating *P. puparum* from *P. apum* females. Females of *P. apum* have at least the metatibia similarly dark mesally as the metafemur (Fig. 5A), whereas females of *P. puparum* have the metatibiae obviously paler than the metafemur (Fig. 11A).

Eight females were borrowed from CBG and confirmed morphologically as *P. puparum*: BIOUG02229-D12 (BOLD ID: MCCA6665-12), BIOUG02448-B07 (BOLD id.: MAMT1549-12), BIOUG05444-A09 (BOLD ID: SSWLB6186-13), BIOUG53912-DO8 (BOLD ID: AACTA4906-20), BIOUG66737-B05 (BOLD ID: GMPOO1141-21), BIOUG66737-B10 (BOLD ID: GMPOO1146-21), BIOUG66737-G01 (BOLD ID: GMPOO1197-21), and BIOUG66784-F04 (BOLD ID: GMPOO5845-21).

Pteromalus quadridentatus Gibson n. sp.

Figs 4B, 13–16

Type material. Holotype (♀, CNC). “CANADA: BC, Chilliwack, Teskey Rd., 49.10453, -21.92742, coll. 19.VII.2020, em. 7.VIII.2020, P. Abram & M. Franklin, *Rubus armeniacus*, #14.1” [BOLD ID: PTAGA036-23]. Condition of holotype: point-mounted; both mandibles exposed; entire except left middle leg missing beyond trochanter (dissected for DNA analysis).

Paratypes (173♀, 71♂ deposited in CNC, NMBe, NHMUK and USNM). CANADA. BRITISH COLUMBIA: *Abbotsford*, 49.071908, -122.340645, coll. 29.VI.2022, J. Sherwood & A. McConkey, *Fragaria*, #AJS23091 [BOLD ID: PTAG054-23] (1♀). *Abbotsford*, Abbotsford Recreation Centre, 49.047636, -122.261520, coll. 21.VI.2022, em. 09.VII.2022, J. Sherwood & A. McConkey, *Dasiphora fruticosa*, #AJS30911 [BOLD ID: PTAGA012-23] (1♀). *Abbotsford*, Clearbrook Substation, 49.011633, -122.337089, Y. Uriel, *Rubus idaeus*—coll. 30.VI.2021, em. 5.VII.2021 (1♀, 1♂); coll. 30.VI.2021, em. 5.VII.2021, #198.3 (1♀); coll. 30.VI.2021, em. 12.VII.2021, #198.4 (1♀). *Abbotsford*, Community Garden, 49.03509, -122.24650, coll. 10.VIII.2021, em. 3.IX.2021, Y. Uriel, *Rubus armeniacus* (1♂). *Agassiz*, 49.241474N, -121.755220W, M. Franklin & P. Abram, coll. 22.VII.2020, em. 3.VIII.2020, aborted raspberry buds (2♀). 49.241474N, -121.755220W, M. Franklin & P. Abram,

aborted cultivated blackberry buds—coll. 20.VII.2020, em. 9.IX.2020 (1♀), coll. 5.VIII.2020, em. 10.VIII.2020 (3♀), coll. 2.IX.2020, em. 7.IX.2020 (1♀), coll. 2.IX.2020, em. 11.IX.2020 (2♀). *Agassiz* (AAFC), 49.2444N, -121.7639W, coll. 20.VIII.2021, em. 14.IX.2021, M. Franklin & P. Abram, Himalayan blackberry buds, Sample #9 (1♀). *Agassiz* (AAFC), 49.243433, -121.754652, M. Franklin, ex. *Rubus armeniacus* buds, 49.243433, -121.754652, M. Franklin, ex. *Rubus armeniacus* buds—coll. 28.VI.2023, em. 13.VII.2023 (3♂), em. 17.VII.2023 (1♀, 2♂), em. 20.VII.2023 (7♀), em. 19.IX.2023 (1♂); coll. 28.VII.2023, em. 15.VIII.2023 (1♀), em. 17.VIII.2023 (1♀, 1♂); coll. 28.VII.2023, em. 11.IX.2023 (1♀); coll. 25.VIII.2023, em. 11.IX.2023 (1♂); coll. 7.IX.2023, em. 3.X.2023 (1♂), em. 20.X.2023 (1♀, 2♂). *Agassiz* (AAFC), 49.243433, -121.754652, M. Franklin, ex. *Rubus idaeus* buds—coll. 22.VI.2023, em. 13.VII.2023 (2♂); coll. 28.VI.2023, em. 17.VII.2023 (2♀, 1♂). *Agassiz*, Agassiz Research & Development Centre, M. Franklin, Himalayan blackberry—coll. 19.VIII.2020, em. 9.IX.2020, Sample ID: AG-BLA-MIX-19-VII-20, Sequence ID: P67-19.04.21 [BOLD ID: PTAGA008-21] (1♀); coll. 2.IX.2020, em. 23.IX.2020, Sample ID: AG-BLA-BB-02-IX-20, Sequence ID: P86 [BOLD ID: PTAGA009-21] (1♀). *Agassiz*, Agassiz Field Station, 49.2444, -121.7639, M. Franklin, *Rubus armeniacus*—coll. 22.VII.2020, em. 10.VIII.2020, #19.2 [BOLD ID: PTAGA037-23] (1♀); coll. 29.VII.2020, em. 3.VIII.2020 (1♀); coll. 29.VII.2020, em. 5.VIII.2020 (1♀); coll. 29.VII.2020, em. 17.VII.2020, #24 [BOLD ID: PTAGA013-23] (1♂); coll. 5.VIII.2020, em. 17.VIII.2020 (1♀); coll. 12.VIII.2020, em. 19.VIII.2020 (1♀); coll. 12.VIII.2020, em. 28.VIII.2020, #40.2 (1♀); coll. 12.VIII.2020, em. 31.VIII.2020 (1♂); coll. 20.VIII.2020, em. 26.VIII.2020, #38.2 [BOLD ID: PTAGA014-23] (1♂); coll. 20.VIII.2020, em. 4.IX.2020, #50 (1♀); coll. 25.VIII.2020, em. 2.IX.2020 (1♀); coll. 2.IX.2020, em. 7.IX.2020 (1♂); coll. 2.IX.2020, em. 11.IX.2020 (1♂), #58.3 (1♂); coll. 2.IX.2020, em. 16.IX.2020, #67.2 (1♀); coll. 9.IX.2020, em. 16.IX.2020 (1♀); coll. 9.IX.2020, em. 29.IX.2020 (1♀), #79.3 (1♂); coll. 16.IX.2020, em. 19.IX.2020 (1♀); coll. 18.IX.2020, em. 21.IX.2020, #72.1 (1♂); em. 2.IX.2022, #544 [BOLD ID: PTAGA027-23] (1♀), #559 [BOLD ID: PTAGA033-23] (1♀), #563 (1♂); em. 14.IX.2022, #551 [BOLD ID: PTAGA030-23] (1♂) #527 [BOLD ID: PTAGA023-23] (1♂); em. 21.IX.2022, #524 (1♀), #532 [BOLD ID: PTAGA025-23] (1♀), #537 (1♀), #545 [BOLD ID: PTAGA053-23] (1♀), #547, [BOLD ID: PTAGA028-23] (1♂), #549 [BOLD ID: PTAGA029-23] (1♂), #553 (1♂), #554 (1♂); em. 22.IX.2022, #528 [BOLD ID: PTAGA024-23] (1♂), #535, Sequence [BOLD ID: PTAGA026-23] (1♀); em. 28.IX.2022, #558 [BOLD ID: PTAGA032-23] (1♀), #564 [BOLD ID: PTAGA034-23] (1♂). *Agassiz*, Agassiz Field Station, 49.2444, -121.7639, M. Franklin, coll. 30.VI.2021, em. 12.VII.2021, *Rubus idaeus* (1♂). *Agassiz*, Agassiz Field Station, 49.2444, -121.7639, 30.VI.2021, Y. Uriel, *Rubus idaeus*—coll. 22.VIII.2020 (1♂); em. 6.VII.2021, #196.2 (1♂); coll. 30.VI.2021, em. 12.VII.2021, #196.40 [BOLD ID: PTAGA016-23] (1♀). *Agassiz*, Agassiz Field Station, 49.2444, -121.7639, M. Franklin & Y. Uriel, *Rubus armeniacus*—em. 02.IX.2022, #518 (1♀), #520 [BOLD ID: PTAGA038-23] (1♀), #533 [BOLD ID: PTAGA051-23] (1♀), #542 [BOLD ID: PTAGA045-23] (1♀); em. 14.IX.2022, #517 [BOLD ID: PTAGA048-23] (1♀), #534 [BOLD ID: PTAGA042-23] (1♀), #536 [BOLD ID: PTAGA043-23] (1♀); em. 21.IX.2022, #519 (1♀), #522 [BOLD ID: PTAGA040-23] (1♀), #529 [BOLD ID: PTAGA041-23] (1♀), #538 [BOLD ID: PTAGA044-23] (1♀), , #543 [BOLD ID: PTAGA052-23] (1♀), #546 [BOLD ID: PTAGA046-23] (1♀). *Burnaby*, 49.2331729, -122.9392711, Jade Sherwood, ex. *Rubus armeniacus*—coll. 15.IX.2021, em. 17.IX.2021, code: BC.Bu.Rubus.15.9.2021_17.9.2021#237_11, reference #10807 (1♀); coll. 15.IX.2021, em. 23.IX.2021, code: BC.Bu.Rubus.15.9.2021_23.9.2021#237_P3A, reference #10817 (1♀); coll. 15.IX.2021, em. 25.IX.2021, code: BC.Bu.Rubus.15.9.2021_25.9.2021#237_12B, reference #10822 (1♀); coll. 15.IX.2021, em. 27.IX.2021, code: C.Bu.Rubus.15.9.2021_27.9.2021#237_11, reference #10823 (1♀). *Burnaby*, 49.2362571, -122.9413394, coll. 30.IX.2022, J. Sherwood, *Rubus armeniacus*, #AJS30638 [BOLD ID: PTAGA062-23] (1♂). *Burnaby*, 49.282101, -123.008770, M. Franklin, ex. *Dasiphora fruticosa* buds, em. 30.VII.2023 (1♀). *Chilliwack*, *Fragaria*—49.104384, -122.006020, coll. 10.VI.2021, em. 7.VII.2021, Y. Uriel, (1♀); 49.107115, -122.003863, coll. 01.VIII.2022, J. Sherwood & A. McConkey, #AJS30373 [BOLD ID: PTAGA059-23] (1♀). *Chilliwack*, J. Sherwood & A. McConkey, *Dasiphora fruticosa*—49.146470, -121.977410, coll. 05.VII.2022, em. 22.VII.2022, #AJS30909 [BOLD ID: PTAGA010-23] (1♀); 49.146000, -121.962440, coll. 12.VIII.2022, em. 24.VIII.2022, #AJS30910 [BOLD ID: PTAGA011-23] (1♀); 49.146000, -121.962440, coll. 12.VIII.2022, em. 26.VIII.2022, #AJS30907 (1♀). *Chilliwack*, Great Blue Heron Reserve, 49.0962, -122.0445, Y. Uriel, ex. *Rubus armeniacus*—coll. 5.VIII.2021, em. 11.VIII.2021, #192.1 (1♀); coll. 5.VIII.2021, em. 16.VIII.2021 (2♀). *Chilliwack*, Great Blue Heron Reserve, 49.0962, -122.0445, M. Franklin, ex. *Rubus armeniacus* buds—coll. 27.VI.2023, em. 10.VII.2023 (2♂), em. 17.VII.2023 (14♀, 2♂), em. 20.VII.2023 (3♀, 2♂); coll. 14.VII.2023, em. 8.VIII.2023 (2♀, 1♂), em. 24.VII.2023 (1♀, 1♂), em. 26.VII.2023 (1♀) em. 31.VII.2023 (1♂); coll. 28.VII.2023, em. 10.VIII.2023 (1♂), em. 17.VIII.2023 (1♀, 1♂), em. 31.VII.2023

(1♀); coll. 9.VIII.2023, em. 28.VIII.2023 (1♀), em. 5.IX.2023 (1♂); coll. 8.IX.2023, em. 11.IX.2023 (1♀), em. 22.IX.2023 (1♂), em. 3.X.2023 (1♂), em. 10.X.2023 (1♀). Great Blue Heron Nature Reserve, 49.095471, -122.045042, J. Sherwood & A. McConkey, *Rosa* sp.—coll. 28.VI.2022, em. 22.VII.2022, #AJS30212 [BOLD ID: PTAGA057-23] (1♂), #AJS30214 [BOLD ID: PTAGA058-23] (1♀); coll. 05.VII.2022, em. 27.VII.2022, #AJS30610 [BOLD ID: PTAGA060-23 (1♂), #AJS30612, [BOLD ID: PTAGA061-23 (1♀); coll. 26.VII.2022, em. 05.VIII.2022, #AJS23219 (1♀). **Chilliwack**, Ryder Lk., 49.097742N, -121.845373W, M. Franklin & P. Abram—coll. 19.VII.2020, em. 5.VIII.2020, aborted cultivated blackberry buds (1♀); coll. 19.VII.2020, em. 31.VIII.2020, aborted Himalayan blackberry buds (1♀). **Chilliwack**, Teskey Rd., 49.10453, -121.92742, coll. 19.VII.2020, em. 5.VIII.2020, M. Franklin, *Rubus armeniacus*, #12 (1♀). Teskey Rd., 49.104564N, -121.927391W, M. Franklin & P. Abram, aborted Himalayan blackberry buds—coll. 19.VII.2020, em. 31.VII.2020 (2♀, 1♂); coll. 19.VII.2020, em. 314.VIII.2020 (1♀, 2♂). Teskey Rd., 49.104564N, -121.927391W, P. Abram, aborted Himalayan blackberry buds—coll. 19.VII.2020, em. 31.VII.2020 (1♀); coll. 19.VII.2020, em. 3.VIII.2020, Sample ID: TESK-BLA-19-VII-20, Sequence ID: 119 [BOLD ID: PTAGA005-21] (1♀); coll. 19.VII.2020, em. 4.VIII.2020 (2♀); coll. 19.VII.2020, em. 5.VIII.2020, Sample ID: TESK-BLA-19-VII-20, Sequence ID: 112-3-HCO2198 [BOLD ID: PTAGA003-21] (1♀). Teskey Rd., 49.104564, -121.927391, P. Abram & M. Franklin, *Rubus armeniacus*—coll. 19.VII.2020, em. 31.VII.2020, #3.3 (1♂); coll. 19.VII.2020, em. 3.VIII.2020, #8.1 [BOLD ID: PTAGA035-23] (1♀), #8.3 (1♀); coll. 19.VII.2020, em. 7.VIII.2020, #14.3 (1♂). **Chilliwack** (WTC), 49.098233N, -121.925255W, coll. 16.VII.2020, em. 07.VIII.2020, M. Franklin & P. Abram, aborted Himalayan blackberry buds (2♀). **Chilliwack**, WT(Promontory), 49.105633, -121.944133, M. Franklin, *Rubus armeniacus*—coll. 16.VII.2020, em. 21.VIII.2020, #31.1 (1♂), #31.2 (1♂); coll. 16.VII.2020, em. 31.VIII.2020, #5 (1♂). **Delta**, Cranberry Research Farm, 49.1021N, -123.0279W, 24.VIII.2021, em. 10.IX.2021, M. Franklin & P. Abram, Himalayan blackberry buds, Sample #10 (2♀). Cranberry Research Farm, 49.1021, -123.0279, M. Franklin, *Rubus armeniacus*—coll. 24.VIII.2021, em. 31.VIII.2021, #202.05 [BOLD ID: PTAGA017-23] (1♂), #202.7 (1♂), #202.08 (1♀). **Delta**, Cranberry Research Farm, 49.1021, -123.0279, Y. Uriel, ex. *Rubus armeniacus*—coll. 17.VIII.2021, em. 1.IX.2021 (1♀, 1♂); coll. 24.VIII.2021, em. 11.VIII.2021 (1♀), #202.02 (1♀); coll. 24.VIII.2021, em. 31.VIII.2021, #203.02 [BOLD ID: PTAGA018-23] (1♂). **Hope**, Ruby Creek, 49.43226425, -121.6377253, M. Franklin, ex. *Rubus armeniacus* buds, coll. 30.VI.2023, em. 18.VII.2023 (1♀). **Langley**, 49.122350, -122.543233, coll. 29.VI.2022, J. Sherwood & A. McConkey, *Fragaria*, #AJS23040 (1♂). **Maple Ridge**, 49.238339, -122.579705, M. Franklin, *Rubus armeniacus*—coll. 3.VIII.2020, em. 24.VIII.2020 (1♀, 1♂), #33.5 (1♀); coll. 6.IX.2020, em. 14.IX.2020 (1♀); coll. 4.VIII.2021, em. 1.IX.2021, #186.03 (1♂); coll. 16.VIII.2021, em. 10.IX.2021, #184.06 [BOLD ID: PTAGA015-23] (1♂). **Maple Ridge**, 49.239411, -122.579158, M. Franklin, ex. *Rubus armeniacus* buds—coll. 27.VI.2023, em. 13.VII.2023 (1♀), em. 20.VII.2023 (3♀); coll. 28.VI.2023, em. 21.VII.2023 (1♂); coll. 14.VII.2023, em. 1.VII.2023 (1♀), em. 20.VII.2023 (4♀), em. 26.VII.2023 (1♀), em. 31.VII.2023 (5♀); coll. 28.VII.2023, em. 8.VIII.2023 (1♀); coll. 11.VIII.2023, em. 17.VIII.2023 (1♀), em. 5.IX.2023 (1♀), em. 19.IX.2023 (1♂); coll. 25.VIII.2023, em. 11.IX.2023 (2♀), em. 19.IX.2023 (1♂); coll. 13.IX.2023, em. 25.IX.2023 (1♀); coll. 23.IX.2023, em. 30.X.2023 (2♀); coll. 13.X.2023, em. 3.X.2023 (1♀, 1♂). **Maple Ridge**, 49.238339, -122.579705, M. Franklin, *Rubus idaeus*—coll. 17.VI.2020, em. 6.VII.2020 (1♂); coll. 17.VI.2020, em. 9.VII.2021, #194.2 (1♂); coll. 1.VII.2021, em. 9.VII.2021, #200 (1♂). **Maple Ridge**, Maple Ridge Park, 49.239411, -122.579158, Y. Uriel, *Rubus armeniacus*—coll. 3.VIII.2020, em. 24.VIII.2020, #33.3 (1♀), #33.6 (1♀); coll. 4.VIII.2021, em. 1.IX.2021, #186.04 (1♀); coll. 23.VIII.2021, em. 10.IX.2021 (1♀), #206.05 [BOLD ID: PTAGA019-23] (1♂), #206.08 [BOLD ID: PTAGA020-23] (1♀); coll. 23.VIII.2021, em. 31.VIII.2021, #206.01 (1♀); coll. 24.VIII.2021, em. 13.IX.2021 (1♀). **Maple Ridge**, 232nd St., M. Franklin, 3.VIII.2020, em. 28.VIII.2020, Himalayan blackberry, Sample ID: MIC-BLA-03-VIII-20, Sequence ID: P48 [BOLD ID: PTAGA007-21] (1♀). 232nd St., M. Franklin, *Rubus armeniacus*—em. 7.X.2022, #523 [BOLD ID: PTAGA022-23] (1♀); coll. 6.X.2022, em. 11.X.2022, #555.00 [BOLD ID: PTAGA031-23] (1♀). **Rosedale**, 49.203395, -121.777829, Y. Uriel, *Rubus armeniacus*—coll. 19.VII.2021, em. 3.VIII.2021 (2♀), #207.2 (1♀), 207.3 [BOLD ID: PTAGA021-23] (1♀). **Yale**, 49.56289765, -121.4339929, M. Franklin, ex. *Rubus armeniacus* buds, coll. 6.VI.2023 (1♂).

USA. WASHINGTON STATE: Sudden Valley, 48.71816149, -122.3416272, ex. Himalayan blackberry buds, Wendy King—coll. 28.VI.2023, em. 12.VII.2023 (1♀); coll. 13.VII, em. 21.VII.2023 (1♀); coll. 8.VIII.2023, em. 22.VIII.2023 (1♀), 31.VIII.2023 (1♀), 9.IX.2023 (1♀).

Diagnosis. FEMALE. Head with POL at least 1.4× OOL (Fig. 15A); lower face laterad clypeus toward malar space and dorsally to about level of lower orbit obliquely strigose to imbricate-reticulate compared to isodiametric

meshlike reticulate parascrobal region (Fig. 14B,F). Antenna with scape comparatively long, extending dorsally at least to level of anterior ocellus (Figs 13A, 14A); flagellum (Fig. 13C,G) with basal funiculars quadrangular to slightly longer than wide and apical funiculars quadrangular to slightly transverse such that combined length of pedicel and flagellum usually only slightly less than, but at least 0.8×, width of head. Fore wing (Fig. 13D) usually with basal fold bare or with only 1–3 setae, though rarely up to 6 setae dorsally, including 1 seta on mediocubital fold or within basal cell apically (Fig. 13H); marginal vein at least 1.4× length of stigmal vein (inner margin obviously longer than stigmal vein) and subequal in length to postmarginal vein. Legs (Fig. 13A,E) with all femora uniformly dark except apically, and metatibia usually partly, variably dark brown except for pale region basally and apically, the basal region about as long as apical pale region of metafemur and apical pale region longer.

MALE. Head with POL conspicuously longer (at least about 1.6×) than OOL (Fig. 15C); lower face obliquely strigose-reticulate to pustulate-imbricate or rugulose laterad clypeus toward malar space and inner orbit dorsally to about level of lower orbit or torulus compared to isodiametric meshlike reticulate parascrobal region and supraclypeal region (Fig. 15E). Antenna (Fig. 15F,G) yellow or pedicel dorsally and each funicular and club brownish basally or basally and dorsally such that flagellum appears brown in dorsal view but at least slightly paler, more yellowish or yellowish-brown ventrally (flagellum can appear more uniformly brown if flagellomeres collapsed or in smaller males, Fig. 15G); scape comparatively elongate-slender similar to female and often with variably conspicuous

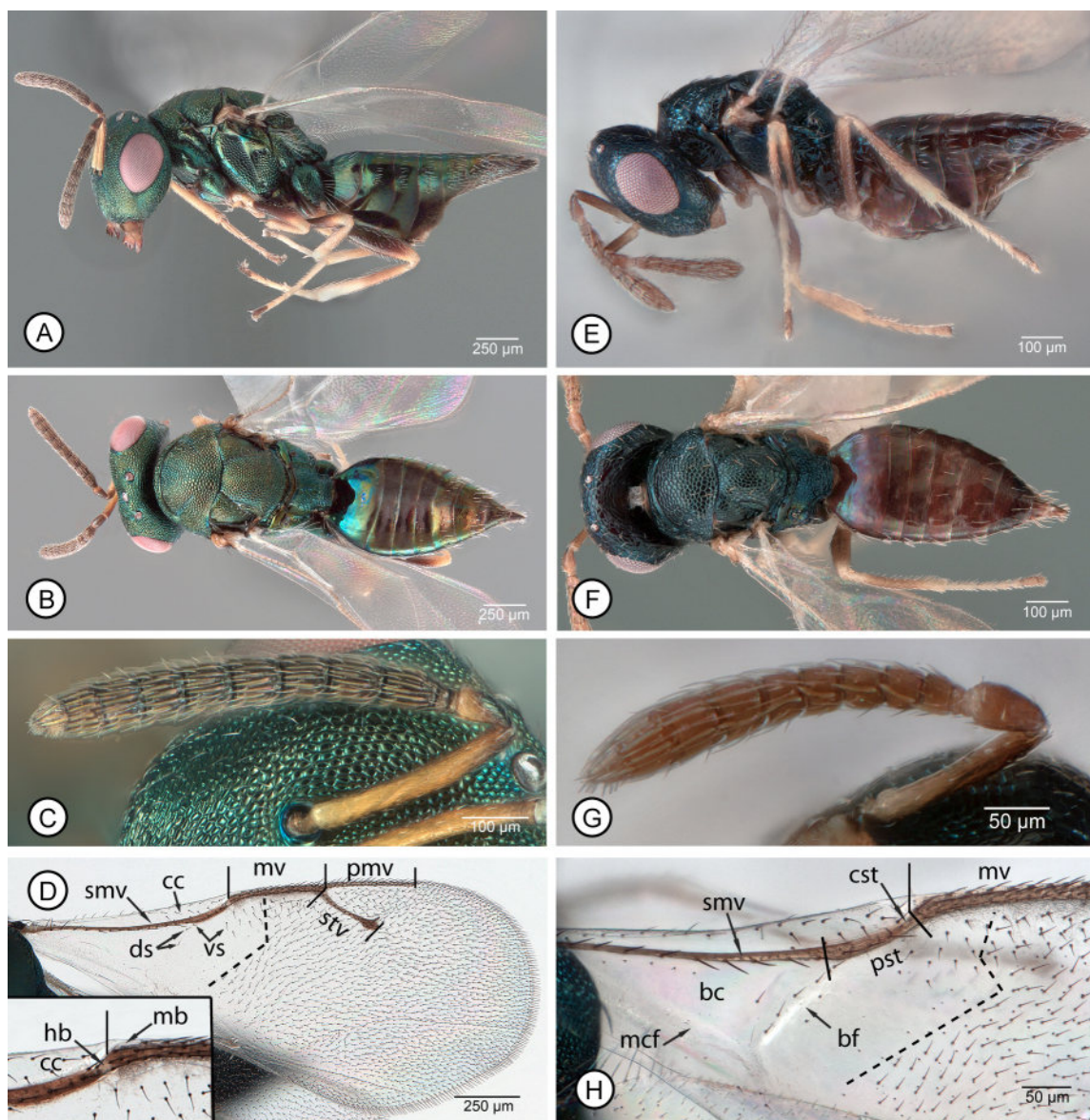


FIGURE 13. *Pteromalus quadridentatus* (♀). **A–D**, typical form: **A**, lateral habitus (holotype); **B**, dorsal habitus (holotype); **C**, antenna; **D**, fore wing (inset: close up of juncture of parastigma and marginal vein). **E–H**, small bodied female: **E**, lateral habitus; **F**, dorsal habitus; **G**, antenna, **H**, basal half of fore wing. See “Methods” for explanation of abbreviations.

paler, convex, slender boss ventroapically (Fig. 15D,F,G); flagellum with funiculars usually obviously oblong (Fig. 15F,G), but if only slightly longer than wide then combined length of pedicel + flagellum subequal in length or longer than width of head. Fore wing (Fig. 16G) with relative lengths of mv, stv and pmv similar to female except length of mv: stv longer, at least 1.5 \times ; basal fold more commonly with 4 or more setae, and rarely up to 11 setae on basal fold and on mediocubital fold and basal cell apically. Legs (Fig. 16A,B) almost always entirely yellow beyond coxae, except for apical tarsomeres, or with metafemur somewhat darker yellowish-orange (Fig. 16B) or rarely variably extensively brown. Gaster usually with complete, broad, encircling yellow band subbasally (Fig. 16A,B), though sometimes appearing entirely dark or with only obscurely paler subbasal band if gaster strongly shrunken/shrivelled (Fig. 16C).

Description. FEMALE. Length, 1.2–[2.7] mm; length of head + mesosoma 1.0–1.2 [1.09] \times length of gaster. Colour. Head capsule, excluding ocelli and pink to grey eyes, usually mostly metallic olive green to somewhat bluish-green, though sometimes with bronze to reddish luster, particularly on upper face and/or vertex along inner orbits under some angles of light, and smaller females sometimes with only quite obscure metallic luster so as to be darker (*cf.* Figs 13A,B with 13E,F). Labiomaxillary complex with palpi dark brown. Mandibles (Figs 3B, 14A) yellowish basally but teeth darker, reddish-brown to brown. Antenna usually with scape yellow or at most brownish dorsoapically, pedicel brown dorsally but yellow ventrally and sometimes apicolaterally, and flagellum contrastingly dark brown except basal anellus usually yellowish (Fig. 13C) but smaller females sometimes with antenna more uniformly yellowish-brown to dark brown (Fig. 13G). Mesosoma similar in colour to head except dorsally sometimes with variably extensive coppery to bronze or reddish luster on mesonotum under some angles of light and propodeum sometimes more distinctly bluish-green, and smaller females sometimes with only quite obscure metallic luster so as to be similarly dark as head; tegula yellow to brownish-yellow (Fig. 15B). Legs (Fig. 13A,E) with coxae same colour as body (Fig. 15B); trochanters and trochantelli pale compared to femora, with trochanters usually somewhat darker, more brownish, than trochantelli; femora with at least about basal three-quarters dark brown and sometimes with slight metallic luster, but pale apically; tibiae sometimes more or less uniformly pale but at least metatibia usually paler basally and apically compared to variably darker, more brownish-yellow to darker brown region subbasally to medially that is at least somewhat paler than respective femur; tarsi pale except apical tarsomeres dark. Wings hyaline with brownish-yellow to light brown venation (Fig. 13D). Gaster (Fig. 13A,B,E,F) brown to black with variably extensive green to bluish-green metallic luster, particularly basally and laterally, and sometimes dark region dorsally with bronze, coppery or reddish-violaceous lusters under different angles of light.

Structure, sculpture and setation. Head in frontal view more or less transverse-quadrangular (Fig. 14A) to subcircular (Fig. 14E), but with genae slightly curved and convergent toward base of mandibles, HH: HW = 0.76–0.89 [0.79]: 1 (HH: HW(B) = 0.72–0.83 [0.73]: 1), and IOD: HW = 0.61–0.66 [0.64]: 1; in dorsal view without occipital carina, 1.1–1.4 [1.23] \times as wide as mesonotum, with HW: HL = 2.0–2.4 [2.3]: 1, POL: OOL = 1.4–1.65 [1.44]: 1 and OOL: LOL = 1.3–1.8 [1.79]: 1; in lateral view MS: EH = 0.5–[0.6]: 1 and EH: EW = 1.3–1.4 [1.39]: 1. Head in frontal view usually with frontovertex, parascrobal region ventrally to about level of lower orbits and, somewhat less coarsely, supraclypeal region, isodiametric mesh-like reticulate, though smaller females sometimes with sculpture finer, more reticulate-coriaceous (shallower) and with comparatively larger cells (*cf.* Fig. 14A,E), but region lateral of clypeus toward malar space and dorsally to about level of lower orbits more obliquely striate-reticulate to imbricate-reticulate (Fig. 14B,F); clypeus (Figs 4B, 14B) with apical margin shallowly incurved, striate to strigose, without depression above emarginate margin; malar space without malar sulcus but with line of differentiated sculpture or narrow band of minute sculpture between lower orbit and base of mandible; gena meshlike reticulate, not carinately margined near base of mandible. Mandibles both quadridentate (Fig. 4B). Labrum smooth and shiny, with one long seta dorsally on either side and one long, apically spatulate seta apically on either side (Fig. 4B) (as illustrated by Darling, 1988, fig. 31, for *P. puparum*). Setae pale, hair-like, inconspicuous. Antennal formula 1:1:2:6:3; inserted slightly above level of lower orbits (Fig. 14A,E) such that distance between dorsal margin of torulus and ventral margin of anterior ocellus subequal in length to distance between ventral margin of torulus and apicolateral margin of clypeus; scape extending dorsally about to level of anterior ocellus or vertex, elongate-tubular, about 5.8–8.9 [7.66] \times as long as greatest width, and about 0.81–[0.92] \times height of eye; length of pedicel + flagellum about 0.0.84–0.95 [0.87] \times head width; pedicel about [1.7]–1.9 \times as long as apical width, about 1.1–1.8 [1.13] \times length of fu1, and about 0.8–1.2 [1.8] \times combined length of anelli and fu1; flagellum usually of similar width along length, though sometimes more distinctly widened apically in smaller females and thus more

distinctly clavate (*cf.* Fig. 13C,G), with width of clava about 1.3–1.8 [1.27]× as wide as ful; funiculars quadrate to slightly longer than wide basally and quadrate to slightly transverse apically (ful about 1.0–1.5 [1.36]× and fu6 about 0.8–1.0 [0.86]× as long as wide), each with comparatively sparse recumbent setae and single row of mps; clava about 2.2–2.9 [2.43]× as long as wide, with 3 distinct segments, each with single row of mps and recumbent setae similar to funiculars, plus a tiny, apical, micropilose sensory region.

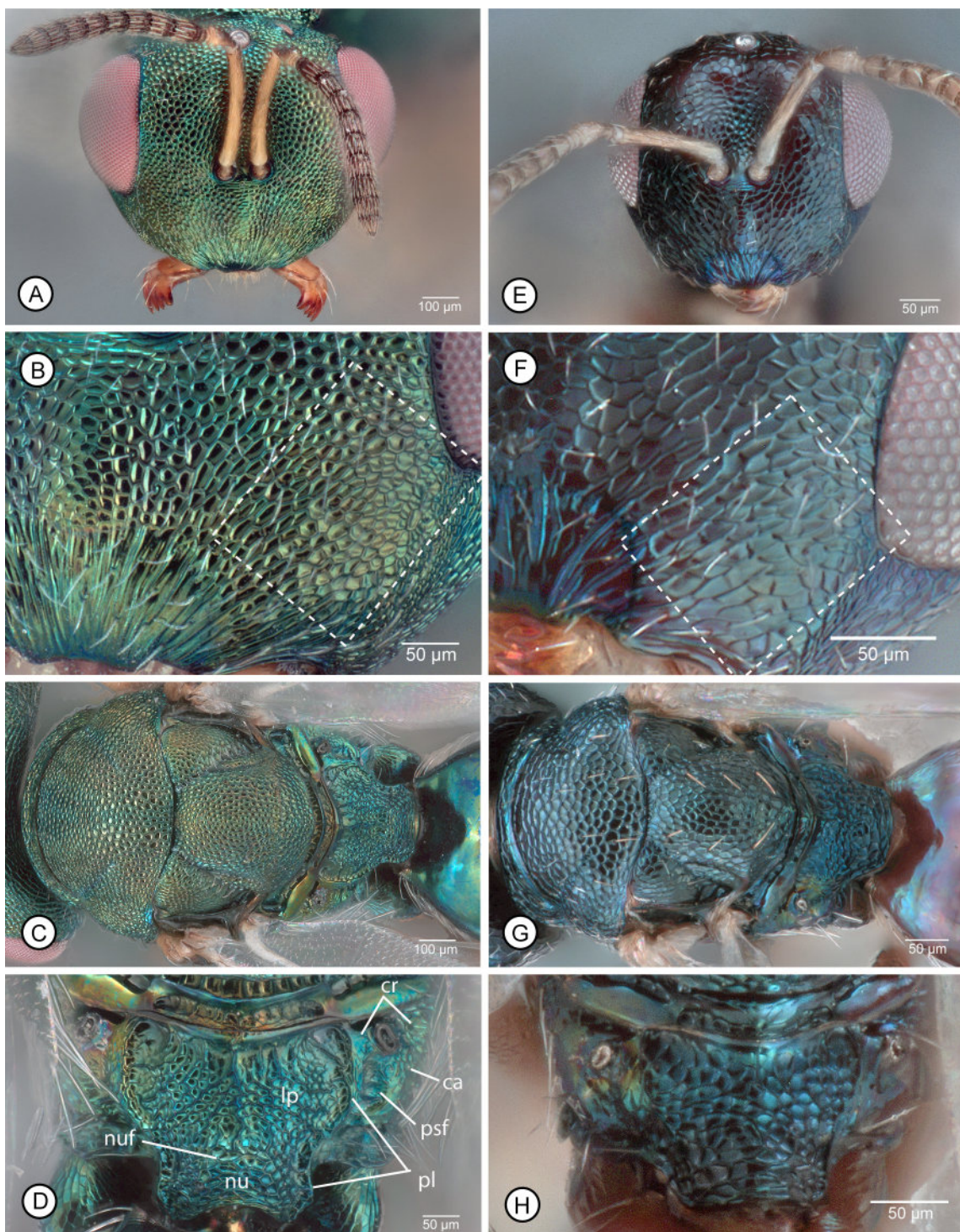


FIGURE 14. *Pteromalus quadridentatus* (♀). **A–D**, typical form: **A**, head, frontal; **B**, lower face, frontolateral; **C**, mesosoma, dorsal; **D**, propodeum. **E–H**, small bodied female: **E**, head, frontal; **F**, lower face, frontolateral; **G**, mesosoma, dorsal; **H**, propodeum. See “Methods” for explanation of abbreviations; dashed line box in **B** and **F** encompass modified region of sculpture.

Mesosoma dorsally (Fig. 14C,G) similarly inconspicuously setose as head, with setae on callus longer, straight, and posteriorly in front of metacoxal flange extending to plica, the setae hairlike and comparatively sparse so as not to obscure cuticle. Pronotum with horizontal collar abruptly angled to neck, with sculpture aligned to produce variably distinct transverse, sometime recurved ridge, but not as a smooth and shiny carina; posterior margin incurved so wider laterally than medially, but medially about 0.1–0.15 [0.13]× length of mesoscutum; collar isodiametric meshlike reticulate except posterior margin transversely alutaceous to smooth and shiny. Mesoscutum isodiametric meshlike reticulate, with cells posteriorly, anterior of scutellar-axillar complex, sometimes slightly larger than more anteriorly or on mesoscutal lateral lobe; about 0.95–1.2 [1.1]× as long as scutellum. Scutellar-axillar complex with axilla isodiametric meshlike reticulate anteriorly to anteromesally, but more obliquely to transversely reticulate or reticulate-imbricate posteriorly and laterally; axillula similar in sculpture to axilla posteriorly, more finely sculptured than dorsally on scutellum; scutellum mostly isodiametric meshlike reticulate, but anteriorly with cells smaller than on mesoscutum posteriorly or on scutellum posteriorly, with frenum at least delineated laterally by smooth, obliquely angled frenal arm and usually dorsomedially either by line of differentiated sculpture between frenal arms or as region of somewhat larger cells; frenum sometimes with inconspicuous differentiated, slender, slightly recurved marginal rim. Metanotum (Fig. 14D,H) consisting laterally of smooth and shiny metascutellar arm posterior to concave, longitudinally crenulate to irregularly sculptured metascutellar trough on either side of dorsellum, with metascutellar arm recurved anteromesally to extend across dorsellum as posteriorly smooth and shiny flange that differentiates dorsellum into similarly long, longitudinally crenulate, transverse furrows, the anterior furrow more strongly sculptured than the posterior furrow though sometimes partly concealed under overlying scutellar apex. Mesosoma laterally (Fig. 15B) not atypically modified, with mesopleuron and metapleuron similarly meshlike reticulate except for smooth and shiny acropleuron and upper mesepimeron or upper mesepimeron finely coriaceous in part (Fig. 15B). Fore wing (Fig. 13D) with marginal vein about 1.4–[1.5]× length of stigmal vein and 1.0–1.1 [1.03]× length of postmarginal vein, with cc: mv: stv: pmv = 2.6–3.2: 1.4–1.5: 1.0: 1.3–1.5 [2.9: 1.5: 1.0: 1.4]; costal cell ventrally with complete line of dark setae along length, including second row apically; bare basally behind entire length of submarginal vein or basal fold with up to 6 dorsal setae including 1 seta on mediocubital fold or within basal cell apically (Fig. 13H), the setal pattern sometimes different on either wing; disc with short marginal fringe and uniformly setose with dark setae except for speculum extending slightly less than half length of marginal vein, the speculum truncate apically (Fig. 13D,H: dashed line); stigmal vein with bulbous but not capitate stigma, and with short uncus with line of 4 campaniform sensilla. Propodeum (Fig. 14D,H) about 0.58–0.68 [0.63]× as long as scutellum (Fig. 14C,G); plicae sinuate, out-curved on either side of lateral panels such that greatest width between plicae about 1.3–1.5 [1.32]× medial length of lateral panels, and curving posteriorly into subparallel or only slightly convergent carinae extending along either side of nucha to posterior margin; nucha convex, meshlike reticulate, including within variably distinct nuchal furrow except often for short median carina, and at least one-third and sometimes up to about one-half length of lateral panels (measurement inexact because line of separation between nucha and panels often not distinct); lateral panels longitudinally crenulate along anterior margin (Fig. 14D), often also variably distinctly transversely sculptured to transversely crenulate laterally near plica, and sometimes with ridges of some sculpture aligned so as to appear partly obliquely strigose but mostly meshlike reticulate as nucha except often with somewhat smaller cells, more punctate-reticulate; with or without median carinae, though if present then usually irregular and often evident only within nuchal furrow or incomplete medially; callar region with comparatively small, oval spiracle usually only narrowly separated from posterior margin of metanotum (Fig. 14D) though by distance up to about maximum diameter of spiracle in some small females (Fig. 14H), and with variably distinct postspiracular furrow (Fig. 14D: psf) usually with one or more internal transverse carinae, though some small females lacking crenulae, and with inner region between spiracle and plica usually more finely sculptured, meshlike coriaceous to coriaceous-reticulate, anteriorly than posteriorly.

Metasoma with smooth and shiny, trapezoidal petiole. Gaster in dorsal view (Fig. 13B,F) lanceolate, about 1.8–2.2 [2.05]× as long as wide; tergites setose laterally, with Gt1 and Gt2 bare, smooth and shiny dorsally, Gt3 usually with setae extending somewhat more extensively dorsomedially but also smooth and shiny, Gt4 usually with complete transverse row of setae though setae often concealed or mostly concealed beneath overlying apex of Gt3 and, if exposed, cuticle finely, isodiametric coriaceous basal to line of setae, and Gt5–synergum more extensively setose and usually more conspicuously, though finely isodiametric coriaceous dorsally; Gt1 with posterior dorsal margin broadly out curved and subsequent tergites with posterodorsal margins similarly broadly out curved to transverse; hypopygium extending about two-thirds length of gaster; ovipositor sheaths extending slightly beyond apex of syntergum.

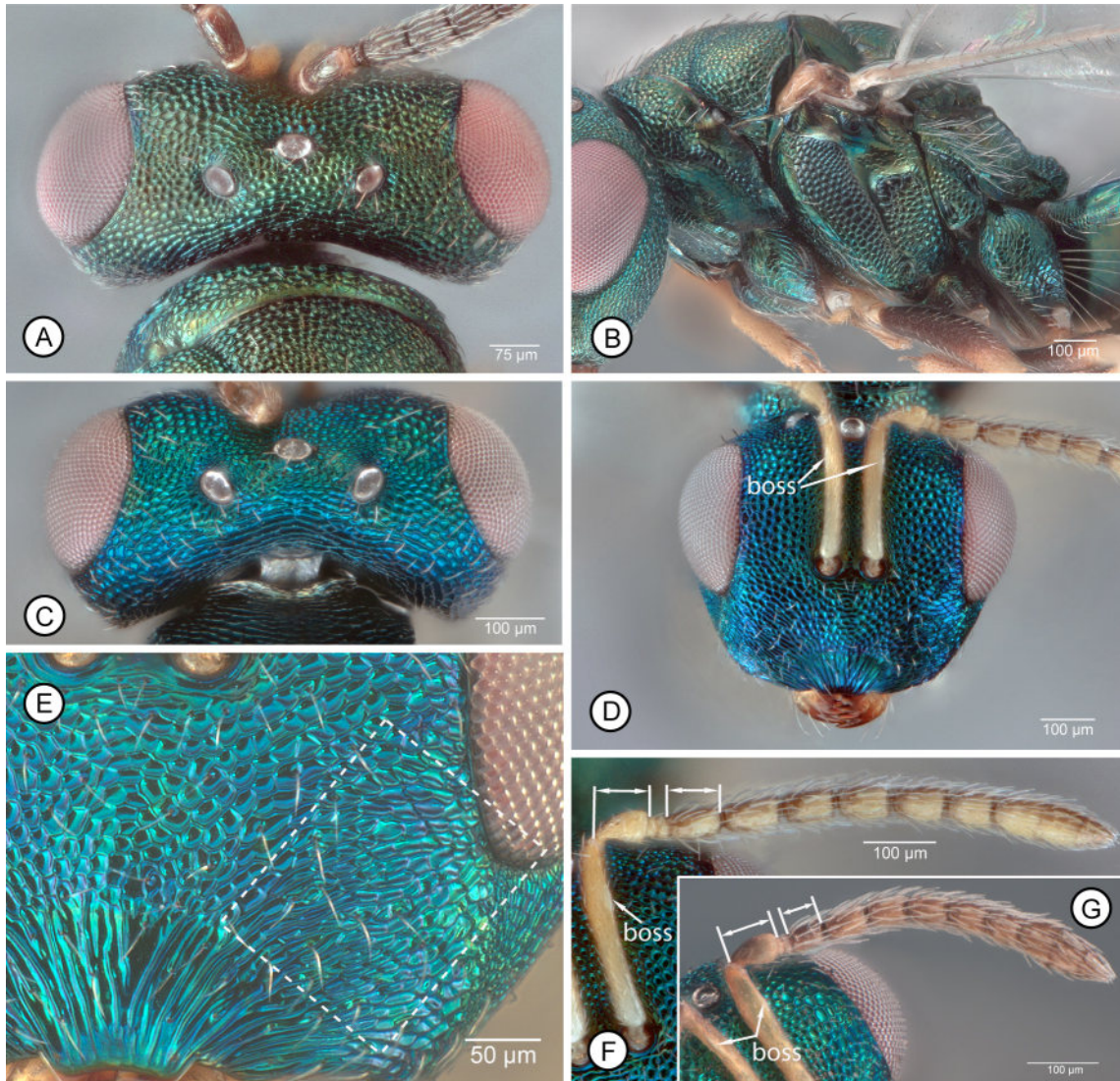


FIGURE 15. *Pteromalus quadridentatus*. **A–B** (♀): **A**, head, dorsal; **B**, mesosoma, lateral. **C–G** (♂): **C**, head, dorsal; **D**, head, frontal; **E**, lower face, frontolateral (dashed line box encompasses modified region of sculpture); **F** and **G**, antenna, lateral (relative lengths of pedicel and ful compared for flagellum of larger (**F**) and smaller (**G**) individual).

MALE. Length, 1.1–2.0 mm. Colour similar to female except as follows: head and mesosoma often with brighter metallic luster, and sometimes more distinctly blue to partly purple in part but without bronze to reddish regions (Fig. 15C–E); antenna entirely yellow or pedicel dorsally and each funicular and club brownish basally or basally and dorsally such that flagellum appears brown in dorsal view but at least slightly paler, more yellowish or yellowish-brown ventrally (Fig. 15F), though flagellum can appear more or less uniformly brown in smaller individuals (Fig. 15G) or if flagellomeres collapsed; labiomaxillary complex with palps yellow; legs (Fig. 16A,B) beyond coxae entirely yellow except for apical tarsomeres or with metafemur somewhat darker yellowish-orange (Fig. 16B) or rarely variably extensively brown; gaster usually with complete, broad, encircling yellow band subbasally over at least apical half of Gt1 and sometimes up to and including Gt3 (Fig. 16A,B), though if gaster shrunken/shrivelled sometimes subbasal band more obscurely orangish-brown or rarely with only obscurely paler region dorsobasally (Fig. 16C: arrow) or essentially entirely dark.

Structure, sculpture and setation. Head similar to female except region lateral of clypeus to level of about lower orbits more conspicuously obliquely strigose to pustulate-imbricate or rugulose (Fig. 15E); head in frontal view (Fig. 15D) with HH: HW = 0.76–0.88: 1, (HH: HW(B) = 0.68–0.85: 1), and IOD: HW = 0.63–0.68: 1; in dorsal view (Fig. 15C) 1.2–1.4× as wide as mesonotum and HW: HL 1.9–2.3: 1, with POL: OOL = 1.6–2.0: 1 and OOL:

$LOL = 1.1\text{--}1.5: 1$; in lateral view $MS: EH = 0.48\text{--}0.61: 1$ and $EH: EW = 1.2\text{--}1.3: 1$. Mandible separated from head capsule by lunate to transversely semicircular membranous region. Antenna with flagellar setation and mps similar to female; scape tubular, about $5.4\text{--}6.7 \times$ as long as wide and about $0.9\text{--}1.0 \times$ length of eye, usually with slender, elongate-oval, slightly paler boss ventroapically (Fig. 15D,F,G: boss), though boss often evident or distinct only in larger individuals; pedicel about $1.5\text{--}2.0 \times$ as long as apical width, about $0.94\text{--}1.7 \times$ as long as fu1, and about $0.75\text{--}1.3 \times$ combined length of anelli and fu1; fu1-fu6 usually obviously oblong and flagellum then appearing filiform (Fig. 15F), but funiculars sometimes only slightly longer than wide and then flagellum appearing more distinctly clavate (Fig. 15G), but with combined length of pedicel + flagellum about $1.0\text{--}1.2 \times$ width of head; fu1 in smaller males rarely only about as long as apical width, though typically appearing at least slightly longer than wide because segment widens apically, with length about $1.0\text{--}2.1 \times$ apical width; fu6 about $1.0\text{--}1.3 \times$ as long as wide; funiculars separated by short pedicel when not collapsed; clava 3-segmented and with tiny, terminal micropilose sensory region similar to female, but clava about $2.8\text{--}3.3 \times$ as long as wide.

Mesosoma (Fig. 16D,E) similar in structure, sculpture and setation to female. Mesosoma with mesoscutum about $1.1\text{--}1.2 \times$ as long as scutellum. Fore wing (Fig. 16G) with mv about $1.5\text{--}1.7 \times$ length of stv and $1.0\text{--}1.2 \times$ length of pmv, with cc: mv: stv: pmv 2.6–2.8: 1.5–1.7: 1.0: 1.3–1.5; setal pattern similar to female except basal fold more commonly with 4 or more setae, and rarely up to 11 setae on basal fold, mediocubital fold, and within basal cell apically. Propodeum (Fig. 16F) similar to female except lateral panels more often with median carina extending to nucha; about $0.57\text{--}0.7 \times$ as long as scutellum, and width between plicae about $1.2\text{--}1.5 \times$ medial length.

Gaster similar in structure, sculpture and setation to female except for secondary sexual features, such that in dorsal view usually more ovate to subcircular (Fig. 16A,C).

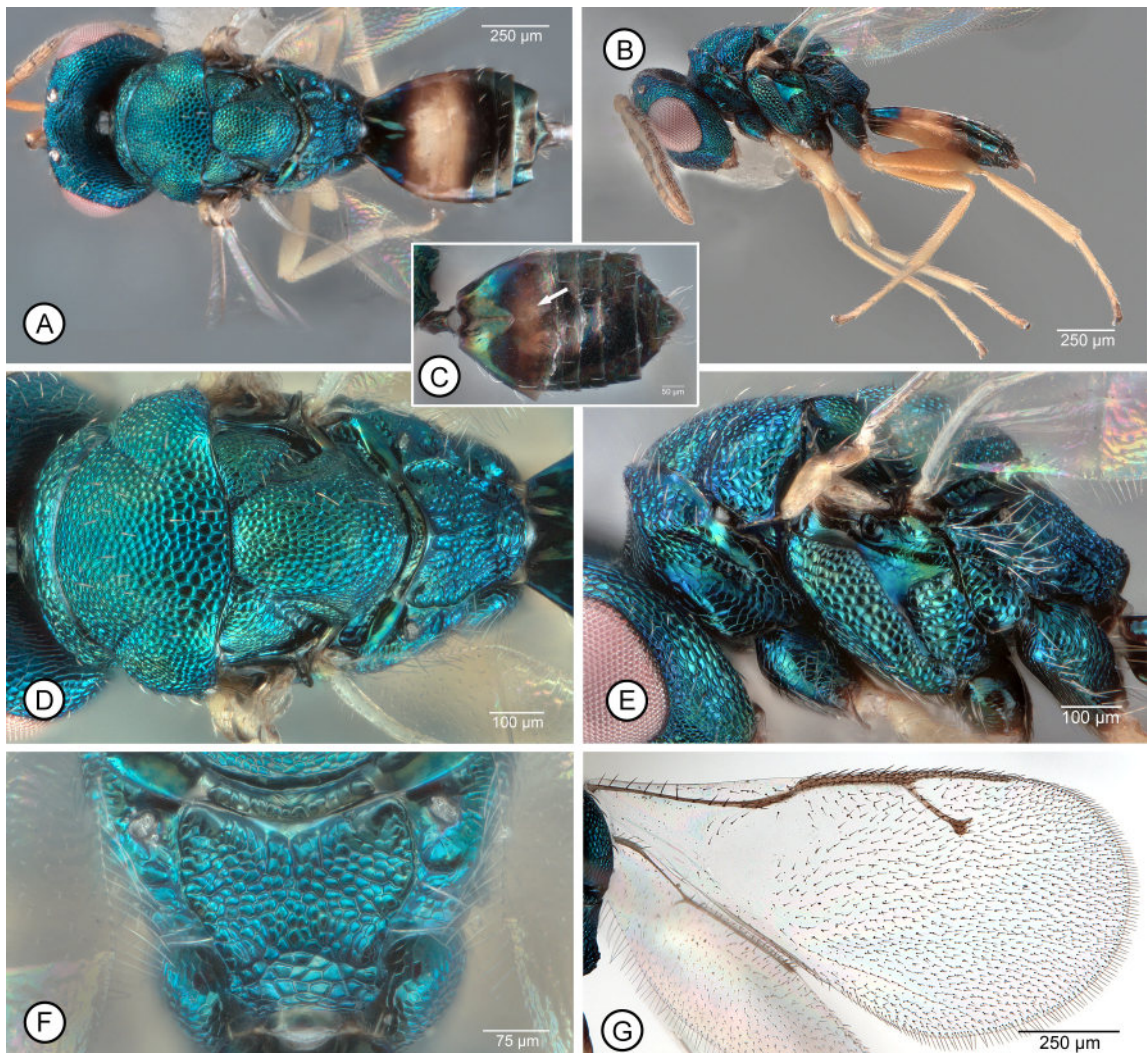


FIGURE 16. *Pteromalus quadridentatus* (♂). A, dorsal habitus; B, lateral habitus; C, gaster, dorsal; D, mesosoma, dorsal; E, mesosoma, lateral; F, propodeum; G, fore wing.

Variation. Some colour, structure and setal features of both sexes appear to be correlated, at least in part, with specimen size. Smaller females usually are comparatively dark with less distinct metallic luster or at least without the other metallic lusters dorsally that are sometimes observed in larger females (*cf.* Figs 13A,B with 13E,F and 14A–D with 14E–H). The head and mesosoma of the smallest specimens have comparatively finer, shallower sculpture with relatively larger cells (*cf.* Figs 14A–D with 14E–H), are more likely to have a greater number of setae on the basal fold (Fig. 13H), and a propodeum with the propodeal plical region somewhat more transverse (*cf.* Figs 14C,D with 14G,H) and the collar region without a distinct postspiracular furrow (*cf.* Fig. 14D,H). Smaller specimens of both sexes also typically have comparatively shorter funicular segments such that the flagellum then sometimes appears somewhat more clavate and, in particular, relative length of fu1 is noticeably shorter in smaller than larger individuals (*cf.* Figs 13C,G and 15F,G). Smaller structures, such as the subapical boss of the male scape (Fig. 15D,F,G), are also less distinct in smaller individuals. However, the size of and whether or not a distinct pale subbasal band is evident on the male gaster (*cf.* Fig. 16A,C) appears to be more correlated with whether or not the gaster is collapsed and shrivelled, though this artefact of preservation is more common for smaller individuals.

Molecular characterization. The average nucleotide composition of *P. quadridentatus* sequences is A = 42.9%, T = 31.1%, C = 12.7%, and G = 13.3%. All *P. quadridentatus* COI sequences showed a high sequence identity, ranging from 99.6 to 100% identical. The relatively small area (120 km by 30 km) where specimens were sampled from could have contributed to the lack of observed COI sequence variation among *P. quadridentatus* specimens.

Etymology. A combination of the Latin prefix *quadri-* (four) and *dentatus* (toothed), in reference to the 4:4 mandibular formula.

Distribution. Canada (British Columbia), USA (Washington State) (Fig. 1).

Biology. Recorded as a solitary, idiobiont larval ectoparasitoid of *A. rubi*. *Pteromalus quadridentatus* larvae feed on paralyzed larvae of *A. rubi* inside closed flower buds. The parasitoid pupates inside the flower bud, and chews a hole through the bud's exterior and exits once developed into an adult. Parasitism of *A. rubi* by this species has been recorded from several host plants belonging to the family Rosaceae, including: strawberries (*Fragaria L. sp.*), raspberries (*Rubus idaeus L.*), Himalayan blackberry (*Rubus armeniacus Focke*), shrubby cinquefoil, (*Dasiphora fruticosa L.*), and Rose (*Rosa spp.*).

This species has been found in agricultural, semi-natural, and urban areas including strawberry fields, hedgerows (Himalayan blackberry), roadsides, public parks, and urban landscaping beds (shrubby cinquefoil; McConkey *et al.* 2023). In Coastal British Columbia, this species has been found on valley bottoms (near sea level) up to 380m above sea level.

Remarks. Both sexes of *P. quadridentatus* are uniquely differentiated from those of other North American species of *Pteromalus* with a 4:4 mandibular formula by sculpture of the lower face lateral of the clypeus not being isodiametric meshlike reticulate and thus dissimilar to the parascrobal region, though this difference is less conspicuous for females than for males. The other four species have the lower face mostly meshlike reticulate except sometimes immediately lateral of the clypeus near the oral margin. An elongate-slender boss ventroapically on the scape will also differentiate males of *P. quadridentatus* males, though this is not distinct or even evident for all males. Females of *P. hemileucae* are similar to those of *P. quadridentatus* except in relative lengths of the fore wing venation, as discussed under the former species. Males of *P. hemileucae* are unknown, but the two putative species also differ biologically, *P. quadridentatus* being the only species of the four that is a solitary parasitoid and a parasitoid of Coleoptera.

Discussion

Our examination of primary type material and/or the original descriptions and subsequent literature on the 59 species of *Pteromalus* recorded from the Nearctic region by Noyes (2019) and phylogenetic analysis of the COI region for 10 species of *Pteromalus* did not result in an available name for the species that we newly describe as *P. quadridentatus*. Further, as part of this study, GAPG examined over 3000 specimens of collected or reared unidentified *Pteromalus* specimens, collected through passive trapping or reared from other host insect species in the CNC from Canada and the USA and did not find a single individual of the new species. However, our study also did not find a potentially conspecific species of *Pteromalus* from elsewhere where *A. rubi* is known, including in Europe where initial rearings from plant hosts infested by *A. rubi* have to date recovered specimens of four

previously described species of *Pteromalus*, but none of our new species (Sherwood 2022). Consequently, it remains to be determined whether *P. quadridentatus* is a native species that has now included *A. rubi* within its host range or whether it was introduced from elsewhere along with *A. rubi* or another non-native insect host. The resolution of this question will require comprehensive faunal surveys and taxonomic revisions of *Pteromalus* in North America and elsewhere from where *A. rubi* is known, but this was beyond the scope of this study.

One important implication of our study is that new species of *Pteromalus* should ideally be described based on large numbers of specimens so that the limits of intraspecific variation can be described accurately. The 245 specimens representing the type series of *P. quadridentatus* include some individuals that are about twice or more as large as others (females 1.2–2.7 mm and males 1.1–2.0 mm). Conspicuous differences in colour (*cf.* Figs 13A,B with 13E,F and 14A–D with 14E–H), sculpture (*cf.* Figs 14A–D with 14E–H), fore wing setal patterns (*cf.* Fig. 13,D,H), and structure of the antennae (*cf.* Figs 13A,D and 15F,G) and propodea (*cf.* Fig. 14D,H) are apparent among the different sized individuals of both sexes. The observed differences might be interpreted as specific differences (e.g. *cf.* Fig. 14A,E) if not for the large number of reared specimens on which *P. quadridentatus* is based, supported by molecular evidence (Fig. 2).

Species limits within the clade of *Pteromalus* that contains *P. quadridentatus* are still not entirely certain. The slightly higher number of COI MOTUs delimited by bPTP compared to ASAP is consistent with other studies that have used these molecular delimitation programs on other chalcidoid families (Sheikh *et al.* 2022; Zhang *et al.* 2022). While testing the species limits of *P. apum* is beyond the scope of our study, we note the result of five MOTUs recovered in our study should be interpreted with caution as many species delimitation software have been shown to over-split the number of true species, and PTP in particular is sensitive to gene flow and other confounding factors such as unbalanced sampling and mutation rate heterogeneity (Luo *et al.* 2018). Finally, our molecular results based on COI have also failed to recover a monophyletic subgenus *P.* (*Pteromalus*) despite morphological support based on mandibular dentition. A comprehensive revision of global *Pteromalus* using an integrative taxonomic approach of detailed morphological study combined phylogenomic scale data is needed in order to resolve this difficult group (Maletti *et al.* 2021).

One of the first steps in the development of a biological control programme is to explore natural enemy associations in the invaded range to identify new associations and/or adventive establishment of natural enemies. The morphological and molecular description of *P. quadridentatus* and differentiation from other North American species *Pteromalus* with a 4:4 mandibular formula is important for the future development of a biological control programme for *A. rubi*. Both sexes of the species can now be accurately distinguished from those of other North American *Pteromalus*. Further, it is now apparent that the presence of *P. quadridentatus* in North America is not the result of an accidental introduction of any known *Pteromalus* with a 4:4 mandibular formula from elsewhere where *A. rubi* is known or any parasitoid in western Europe that is currently known to parasitize *A. rubi* (Sherwood 2022). Consequently, the latter species are candidates for classical (= importation) biological control in North America. The formal description of *P. quadridentatus* will also help to document its biological control impact in North America as an integrated pest management program is developed for *A. rubi*.

Acknowledgements

We thank Natalie Dale-Skey (NHMUK) for providing images of the type material of *P. cassotis* and Joseph Moisan-De Serres (Ministère de l’Agriculture, des Pêcheries et de l’Alimentation du Québec, Québec, Canada) and Valérie Boulva (Université Laval, Québec, Canada) for images of the lectotypes of *P. fuscipes* and *P. melanicus*. We also thank Jeremy deWaard and Renee Miskie for the loan of CBG specimens, Valérie Lévesque-Beaudin for obtaining BOLD records, and Lingfei Peng (Fujian Agriculture and Forestry University, Fuzhou, China) for providing reproductions of and English translations of species descriptions of species of *Pteromalus* described from China in Chinese. We thank Aysha McConkey and Warren Wong (Agriculture and Agri-Food Canada) and Wendy King and Chris Looney (Washington State Department of Agriculture) for their help collecting flower buds for parasitoid emergence and Camille Coray from the Great Blue Heron Nature Reserve in Chilliwack, British Columbia for providing access for specimen collection. Lastly, we thank Paul Adams, Lyndsey Baillie, and Taylor Chin (Applied Genomic Centre, Kwantlen Polytechnic University) for their technical assistance with sequencing specimens. This research was supported by Agriculture and Agri-Food Canada A-base #3884 to M.T.F.

References

- Alonso-Zarazaga, M.A., Barrios, H., Borovec, R., Bouchard, P., Caldara, R., Colonnelli, E., Gültekin, L., Hlavač, P., Korotyaev, B., Lyal, C.H.C., Machado, A., Meregalli, M., Pierotti, H., Ren, L., Sánchez-Ruiz, M., Sforzi, A., Silfverberg, H., Skuhrovec, J., Trýzna, M., Velázquez de Castro, A.J. & Yunakov, N.N. (2017) Cooperative Catalogue of Palaearctic Coleoptera Curculionoidea. *Monografías electrónicas S.E.A.*, 8, 1–729.
- Anonymous (2021) *Anthonomus rubi* (strawberry blossom weevil) – Fact sheet. Online. Available from: <https://inspection.canada.ca/plant-health/invasive-species/insects/strawberry-blossom-weevil/fact-sheet/eng/1632774012031/1632774012719> (accessed 5 August 2024)
- Askew, R.R. & Shaw, M.R. (1997) *Pteromalus apum* (Retzius) and other pteromalid (Hym.) primary parasitoids of butterfly pupae in Western Europe, with a key. *Entomologist's Monthly Magazine*, 133, 67–72.
- Baur, H. (2015) Pushing the limits – two new species of *Pteromalus* (Hymenoptera, Chalcidoidea, Pteromalidae) from Central Europe with remarkable morphology. *ZooKeys*, 514, 43–72.
<https://doi.org/10.3897/zookeys.514.9910>
- Bouček, Z. (1972) On European Pteromalidae (Hymenoptera): a revision of *Cleonymus*, *Eunotus* and *Spaniopus*, with descriptions of new genera and species. *Bulletin of the British Museum (Natural History)*, Entomology, 27, 267–315.
- Bouček, Z. & Graham, M.W.R. de V. (1978) British Check-list of Chalcidoidea (Hymenoptera): taxonomic notes and additions. *Entomologist's Gazette*, 29, 225–235.
- Burks, B.D. (1975) The species of Chalcidoidea described from North America north of Mexico by Francis Walker (Hymenoptera). *Bulletin of the British Museum (Natural History)*, Entomology, 32, 139–170.
- Burks, B.D. (1979) Torymidae (Agaoninae) and all other families of Chalcidoidea (excluding Encyrtidae). In: Krombein, K.V., Hurd, P.D. Jr., Smith, D.R. & Burks, B.D. (Eds.), *Catalog of Hymenoptera in America North of Mexico*. Vol. 1. Smithsonian Institute Press, Washington, D.C., pp. 748–1043.
- Burks, R.A., Mitroiu, M-D., Fusu, L., Heraty, J.M., Jansta, P., Heydon, S., Papilloud, N.D-S., Peters, R.S., Tselikh, E.V., Woolley, J.B., van Noort, S., Baur, H., Cruaud, A., Darling, C., Haas, M., Hanson, P., Krogmann, L. & Rasplus, J.-Y. (2022) From hell's heart I stab at thee! A determined approach towards a monophyletic Pteromalidae and reclassification of Chalcidoidea (Hymenoptera). *Journal of Hymenoptera Research*, 94, 13–88.
<https://doi.org/10.3897/jhr.94.94263>
- Christ, J.L. (1791) *Naturgeschichte, Klassification un nomenclatur der Insekten vom Beinen-, Wespen un Ameisengeschlecht, als der fünften Ordnung des Linneischen Natursystems von den Insekten: Hymenoptera. Mit hätigen Flügeeln.* in der Hermannischen Buchhandlung, Frankfurt a.m., 535 pp.
<https://doi.org/10.5962/bhl.title.87724>
- Doğanlar, M. (1980) A new species of *iyeSwederus* (Hymenoptera; Pteromalidae) from Western Canada. *Türkiye Bitki Koruma Dergisi*, 4, 155–160.
- Dzhankokmen, K.A. (1998) Review of pteromalids of the genus *Pteromalus* Swederus (Hymenoptera, Pteromalidae) from Kazakhstan: I. *Entomological Review*, 78, 706–717. [translated from *Entomologicheskoe Obozrenie*, 77, 483–496]
- Dzhankokmen, K.A. (2001) Review of pteromalids of the genus *Pteromalus* Swederus (Hymenoptera, Pteromalidae) from Kazakhstan: II. *Entomological Review*, 81, 75–97. [translated from *Entomologicheskoe Obozrenie*, 80, 472–496]
- Fabricius, J.C. (1804) *Systema Piezatorum*. Vol. 2. A.C. Reichard, Brunsvigae, xiv + 30 + 440 pp..
- Fourcroy, A.F. de (1785) *Entomologia Parisiensis, sive catalogus Insectorum, quae in agro parisiensi reperiuntur - secundum methodam Geoffraeriam in sectiones, genera et species distributii; cui addita sunt nomina trivialia et fere recentiae novae species.* s.n., Paris, 311 pp.
<https://doi.org/10.5962/t.174486>
- Franklin, M.T., Hueppelsheuser, T.K., Abram, P.K., Bouchard, P., Anderson, R.S. & Gibson, G.A.P. (2021) The Eurasian strawberry blossom weevil, *Anthonomus rubi* (Herbst, 1795), is established in North America. *The Canadian Entomologist*, 153, 578–585.
<https://doi.org/10.4039/tce.2021.28>
- Gibson, G.A.P. (2020) Redescription of *Anastatus mantoidae* Motschulsky, the type species of *Anastatus* Motschulsky 1859, and *Anastatus echidna* (Motschulsky), the type species of *Cacotropia* Motschulsky 1863, with respect to taxonomy of *Anastatus* (Hymenoptera: Eupelmidae: Eupelminae). *Zootaxa*, 4748 (3), 485–513.
<https://doi.org/10.11646/zootaxa.4748.3.5>
- Gibson, G.A.P. (2021) Revision of the Old World genus *Mesocomys* Cameron (Hymenoptera: Eupelmidae). *Zootaxa*, 4901 (1), 1–92.
<https://doi.org/10.11646/zootaxa.4901.1.1>
- Gijswijt, M.J. (1984) *Pteromalus ellisorum*, a new species from the Canary Islands (Hymenoptera: Chalcidoidea, Pteromalidae). *Entomologische Berichten*, 44, 62–64.
- Girault, A.A. (1917) The North American species of *Habrocytus* (Chalcid-Flies). *The Canadian Entomologist*, 49, 178–182.
<https://doi.org/10.4039/Ent49178-5>
- Graham, M.W.R. de V. (1969) The Pteromalidae of north-western Europe (Hymenoptera: Chalcidoidea). *Bulletin of the British Museum (Natural History)*, Entomology, Supplement 16, 1–908.
<https://doi.org/10.5962/p.258046>

- Graham, M.W.R. de V. (1992) Two new species of European Pteromalidae (Hym., Chalcidoidea). *Entomologist's Monthly Magazine*, 128, 115–117.
<https://doi.org/10.1163/187631279X00321>
- Hedqvist, K.J. (1979) Two new species of the genus *Pteromalus* Swed. from Sweden (Hymenoptera: Chalcidoidea: Pteromalidae). *Entomologica Scandinavica*, 10, 155–157.
- Howard, L.O. (1889) The Hymenopterous parasites of North American Butterflies including a section upon the miscogasters by C.V. Riley. In: Scudder, S.H. (Ed.), *The Butterflies of the Eastern United States and Canada, with special reference to New England*. The author, Cambridge, Massachusetts, pp. 1869–1911.
- Hoang, D.T., Chernomor, O., von Haeseler, A., Minh, B.Q. & Le, S.V. (2018) UFBoot2: Improving the ultrafast bootstrap approximation. *Molecular Biology and Evolution*, 35 (2), 518–522.
<https://doi.org/10.1093/molbev/msx281>
- Huang, D.W., Liao, D.X. & Niu, Y.Z. (1987) Studies on pteromalids from insect pests of poplar from Shuoxian County, Shanxi Province. *Sinozoologica*, 5, 155–160.
- Janzon, L.-Å. (1977) *Habrocytus canariensis* n.sp. from Tenerife (Hymenoptera : Chalcidoidea : Pteromalidae). *Entomologica Scandinavica*, 8, 231–232.
<https://doi.org/10.1163/187631277X00305>
- Jurine, L. (1807) *Nouvelle méthode de classer les Hyménoptères et les Diptères. Vol. 1.* Chez J.J. Paschoud, Geneve, 320 + 4 pp., 14 pls.
<https://doi.org/10.5962/bhl.title.60886>
- Kalyaanamoorthy, S., Minh, B.Q., Wong, T.K., von Haeseler, A. & Jermiin, L.S. (2017) ModelFinder: fast model selection for accurate phylogenetic estimates. *Nature Methods*, 14 (6), 587.
<https://doi.org/10.1038/nmeth.4285>
- Klimmek, F. & Baur, H. (2018) An interactive key to Central European species of the *Pteromalus albipennis* species group and other species of the genus (Hymenoptera: Chalcidoidea: Pteromalidae), with the description of a new species. *Biodiversity Data Journal*, 6, e27722.
<https://doi.org/10.3897/BDJ.6.e27722>
- Koponen, M. & Askew, R.R. (2002) Chalcids from Madeira, Canary Islands and Azores (Hymenoptera, Chalcidoidea). *Vieraea*, 30, 115–145.
- Liao, D.X. (1982) Hymenoptera: Chalcidoidea. *Insects of Xizang*, 2, 355–370.
- Liao, D.X., Li, X.L., Pang, X.F. & Chen, T.L. (1987) Hymenoptera: Chalcidoidea (1). *Economic Insect Fauna of China*, 34, i–x + 1–241.
- Linnaeus, C. (1758) *Systema naturae. 10th Edition.* Impensis Direct. Laurentii Salvii, Stockholm, 824 + iii pp.
- Luo, A., Ling, C., Ho, S.Y. & Zhu, C.D. (2018) Comparison of methods for molecular species delimitation across a range of speciation scenarios. *Systematic Biology*, 67 (5), 830–846.
<https://doi.org/10.1093/sysbio/syy011>
- Maletti, S., Niehuis, O., Mayer, C., Sann, M., Klopstein, S., Nottebrock, G., Baur, H. & Peters, R.S. (2021) Phylogeny, taxonomics, and ovipositor length variation of the *Pteromalus albipennis* species group (Hymenoptera: Chalcidoidea: Pteromalidae: Pteromalinae). *Journal of Zoological Systematics and Evolutionary Research*, 59, 349–358.
<https://doi.org/10.1111/jzs.12433>
- McConkey, A., Uriel, Y., Sherwood, J., Wong, W., Hueppelsheuser, T. & Franklin, M. (2023) The invasive strawberry blossom weevil, *Anthonomus rubi* Herbst (Coleoptera: Curculionidae), uses *Dasiphora fruticosa* for reproduction in British Columbia. *Journal of the Entomological Society of British Columbia*, 120. [published online]
- Minh, B.Q., Schmidt, H.A., Chernomor, O., Schrempf, D., Woodhams, M.D., Von Haeseler, A. & Lanfear, R. (2020) IQ-TREE 2: New models and efficient methods for phylogenetic inference in the genomic era. *Molecular Biology and Evolution*, 37 (5), 1530–1534.
<https://doi.org/10.1093/molbev/msaa015>
- Nees von Esenbeck, C.G. (1834) *Hymenopterorum Ichneumonibus affinium, Monographiae, genera Europaea et species illustrantes. Vol. 2.* J.G. Cottae, Stuttgart und Tübingen, 448 pp.
<https://doi.org/10.5962/bhl.title.26555>
- Noyes, J.S. (2019) Universal Chalcidoidea Database. Online. Available from: <https://www.nhm.ac.uk/chalcidooids> (accessed 15 December 2023)
- Provancher, L. (1881) Faune Canadienne. Les Insectes.—Hyménoptères. *Le Naturaliste Canadien*, 12, 289–304.
- Puillandre, N., Brouillet, S. & Achaz, G. (2021) ASAP: assemble species by automatic partitioning. *Molecular Ecology Resources*, 21 (2), 609–620.
<https://doi.org/10.1111/1755-0998.13281>
- Rahmani, Z., Rakhshani, E., Lotfalizadeh, H. & Mokhtari, A. (2022) Annotated checklist of Pteromalidae (Hymenoptera, Chalcidoidea) in the Middle East and North Africa. *Journal of Insect Biodiversity and Systematics*, 8, 265–377.
<https://doi.org/10.52547/jibs.8.2.265>
- Retzius, A.J. (1783) *Caroli DeGeer genera et species Insectorum.* Apud Siegfried Lebrecht Crusium, Lipsiae, 6 + 220 pp.
- Roueché, N.D., Wilson, T.M., Looney, C. & Chamorro, M.L. (2022) *Anthonomus rubi* (Herbst) (Coleoptera: Curculionidae) is established in Washington State and the United States of America. *Proceedings of the Entomological Society of Washington*,

- 124, 367–371.
<https://doi.org/10.4289/0013-8797.124.2.367>
- Sheikh, S.I., Ward, A.K., Zhang, Y.M., Davis, C.K., Zhang, L., Egan, S.P. & Forbes, A.A. (2022) *Ormyrus labotus* (Hymenoptera: Ormyridae): another generalist that should not be a generalist is not a generalist. *Insect Systematics and Diversity*, 6 (1), 8.
<https://doi.org/10.1093/isd/ixac001>
- Sherwood, J. (2022) *Anthonomus rubi* and associated parasitoids. Online. Available from: <https://piee-lab.landfood.ubc.ca/research/anthonomus-rubi-and-associated-parasitoids> (accessed 5 August 2024)
- Spinola, M. (1808) n.k. *Insectorum Liguria species novae aut rariores, quas in agro ligustico nuper detexit, et iconibus illustratavit*, 2 (2–4), 209–262 + v, synoptic table.
- Stenoien, C., McCoshum, S., Caldwell, W., De Anda, A. & Oberhauser, K. (2015) New reports that Monarch butterflies (Lepidoptera: Nymphalidae, *Danus plexippus* Linnaeus) are hosts for a pupal parasitoid (Hymenoptera: Chalcidoidea, *Pteromalus cassotis* Walker). *Journal of the Kansas Entomological Society*, 88, 16–26.
<https://doi.org/10.2317/JKES1402.22.1>
- Swederus, N.S. (1795) Beskrifning på et nytt genus *Pteromalus* ibland Insecterna, haerande til Hymenoptera, uti herr arch. och ridd. v. Linnés Systema Naturae. *Kungliga Svenska Vetenskapsakademiens Handlingar*, 16, 201–205.
- Thomson, C.G. (1878) *Hymenoptera Scandinaviae* 5. *Pteromalus* (*Svederus*) continuation. typis expressit H. Ohlsson, Lundae, 307 pp., 1 pl., Lund.
- Tselikh, E.V. (2020) New data on the pteromalid wasps (Hymenoptera, Chalcidoidea: Pteromalidae) of Eastern Siberia with description of a new genus. *Entomological Review*, 100, 714–726.
<https://doi.org/10.1134/S0013873820050127>
- Untergasser, A., Cutcutache, I., Koressaar, T., Ye, J., Faircloth, B.C., Remm, M. & Rozen, S.G. (2012) Primer3—new capabilities and interfaces. *Nucleic acids research*, 40 (15), e115.
<https://doi.org/10.1093/nar/gks596>
- Vikberg, V. (1979) *Pteromalus bottnicus* sp. n. from North Finland (Hymenoptera, Pteromalidae). *Notulae Entomologicae*, 59, 65–67.
- Vikberg, V. & Askew, R.R. (2006) *Ichneumon cyniphidis* Linnaeus, 1758 belongs to *Pteromalus* Swederus (Hym., Pteromalidae). *Entomologist's Monthly Magazine*, 142, 185–188.
- Walker, F. (1835) Monographia Chalciditum. (Continued.) *Entomological Magazine*, 2, 476–502.
- Walker, F. (1847) XLIV.—Characters of undescribed Chalcidites collected in North America by E. Doubleday Esq., and now in the British Museum. *Annals and Magazine of Natural History*, 19, 392–398.
<https://doi.org/10.1080/037454809494566>
- Yang, Z.Q., Yao, Y.X. & Cao, L.M. (2015) *Chalcidoidea parasitizing forest defoliators* (Hymenoptera). Science Press, Beijing, vii + 283 pp., 21 pls.
- Yao, Y.X. & Yang, Z.Q. (2008) Three species of genus *Pteromalus* (Hymenoptera: Pteromalidae) parasitizing *Rhynchaenus empulifolius* (Coleoptera: Curculionidae), with description of a new species from China. *Scientia Silvae Sinicae*, 44, 90–94.
- Zhang, J., Kapli, P., Pavlidis, P. & Stamatakis, A. (2013) A general species delimitation method with applications to phylogenetic placements. *Bioinformatics*, 29 (22), 2869–2876.
<https://doi.org/10.1093/bioinformatics/btt499>
- Zhang, Y.M., Sheikh, S.I., Ward, A.K., Forbes, A.A., Prior, K.M., Stone, G.N., Gates, M.W., Egan, S.P., Zhang, L., Davis, C., Weinersmith, K.L., Melika, G. & Lucky, A. (2022) Delimiting the cryptic diversity and host preferences of *Sycophila* parasitoid wasps associated with oak galls using phylogenomic data. *Molecular Ecology*, 31 (16), 4417–4433.
<https://doi.org/10.1111/mec.16582>

Supplementary Materials. The following supporting information can be downloaded at the DOI landing page of this paper:

Table S1. Sample information for specimens included in the phylogenetic analysis, including: species, country collected, collection location, BOLD or GenBank accession number, identifier, and specimen storage location, when available.

© Copyright Act of Canada, owned by His Majesty the King in Right of Canada—that is, by the Government of Canada, as represented by the Minister of Agriculture and Agri-Food.